

Review

Architectural Glass under Climatic Actions and Fire: Review of State of the Art, Open Problems and Future Perspectives

Laura Galuppi ^{1,§}, Annalisa Franco ^{2,§} and Chiara Bedon ^{3,*,§}

¹ Department of Engineering and Architecture, University of Parma, 43121 Parma, Italy; laura.galuppi@unipr.it

² Construction Technologies Institute of the Italian National Research Council (ITC-CNR),
20098 San Giuliano Milanese, Italy; annalisa.franco@itc.cnr.it

³ Department of Engineering and Architecture, University of Trieste, Via Valerio 6/1, 34172 Trieste, Italy

* Correspondence: chiara.bedon@dia.units.it; Tel.: +39-040-558-3837

§ The authors contributed equally to this work.

Abstract: A critical issue in the design of structural glass elements in buildings is represented by the evaluation of thermally induced stresses and strains. For both climatic actions and fire, thermal stresses represent one of the main causes of premature failure, due to the high sensitivity of glass to temperature gradients. Thermal loads pose a severe safety risk for glass, due to their uneven distribution but also the lack of knowledge on the modification of mechanical properties with temperature. In design practice, approximate tools are used to describe temperature fields in glazing, which do not adequately estimate the thermally induced stresses. Additionally, the existing standards prescribe different methods for the calculation of both the temperature field and the consequent stress, usually based on strong simplifying assumptions, and there is a lack of uniformly defined procedures. Here, an accurate review of the state of the art on glass elements exposed to thermal actions, from both the scientific and the regulatory perspectives, is presented. Reference is made first to the evaluation of the thermal actions, and further to the proper assessment of both the temperature distribution and the consequent thermal stress. The paper also emphasizes open problems and future perspectives related to these topics, to evidence areas of research that should be strengthened and possible future enhancements to the current design and assessment methodologies, which should also be introduced in a regulatory framework.



Citation: Galuppi, L.; Franco, A.; Bedon, C. Architectural Glass under Climatic Actions and Fire: Review of State of the Art, Open Problems and Future Perspectives. *Buildings* **2023**, *13*, 939. <https://doi.org/10.3390/buildings13040939>

Academic Editor: Xing Jin

Received: 13 March 2023

Revised: 26 March 2023

Accepted: 30 March 2023

Published: 1 April 2023



Copyright: © 2023 by the authors. Licensee MDPI, Basel, Switzerland. This article is an open access article distributed under the terms and conditions of the Creative Commons Attribution (CC BY) license (<https://creativecommons.org/licenses/by/4.0/>).

Keywords: climatic actions; experiments; facades; fire; glass; modelling; standards; thermal shock

1. Introduction

The building skin, delimiting the indoor space and defining the aesthetic appeal of the building itself, plays a definite role in terms of the energy transfer between the inside and outside. The glazing system, the only part of the building that can achieve direct solar gains due to its transparency, is often considered the most critical, particularly for the large, glazed surfaces that are commonly used in prestigious buildings. However, a proper thermal design of the glazing elements, including their sizing and orientation, as well as the use of proper optical and thermal coatings, may help to achieve a positive contribution in terms of energy efficiency and thermal comfort inside the building, as well as natural lighting, outdoor visuals, and natural ventilation. Because of this, the glazed part of the building envelope receives a high level of consideration by architects and engineers [1–3]. Special attention is required in design and maintenance against several types of loads, including mechanical actions and thermal loads [4]. Indeed, the intrinsic properties of glass, together with the typically limited thickness-to-size ratios for glazing elements, make glass structures highly vulnerable.

The “climatic actions” related to solar radiation and heat exchange with the environment [5,6] can produce an uneven temperature distribution in glazing panels, enhanced by the presence of shadows, as well as heat sources such as radiators, hot air outlets, etc. Both

the technical literature and practical experience provide a wealth of evidence that the strain and stress state produced by these temperature differences can lead to failures.

Since glass has relatively poor heat conduction properties, the diverse heating of different regions of the panel (particularly shaded and not-shaded parts) results in temperature gradients on its surface. The thermal expansion/contraction of the hotter/colder regions, enhanced by the high thermal expansion coefficient of glass, give rise to differential thermal strains that, in some cases, cannot be accommodated by clearance of the supports. Furthermore, since the plate contour is usually covered by a frame, preventing the solar radiation from hitting the panel, this usually presents a low temperature. This results in the simultaneous mechanical action of the central part, which is trying to expand, and of the edge region trying to withstand this expansion. As schematized in Figure 1a, this presents compressive stress in the warm part and tensile stress in the colder one. As glass is a fragile material, with a low ability to resist the propagation of flaws, this kind of action makes it prone to thermal cracks [7].

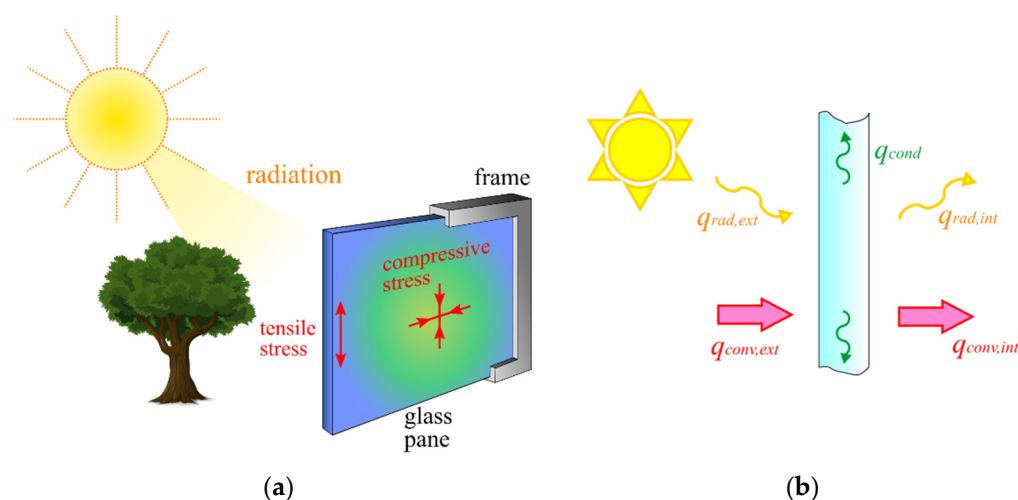


Figure 1. Schematics of (a) typical thermal stress state for a glass window and (b) heat exchange phenomena occurring in a glazing panel due to climatic actions.

This is why the design of glass panes under time-varying climatic loads, specifically solar radiance and environmental temperatures [6,8], represents a key aspect that is often overlooked in practice. The thermal state and the consequent thermal stresses depend on a large number of environmental parameters [9], such as time-dependent internal and external temperatures and solar radiance, as well as on the geometrical and thermo-mechanical properties of the glazing system. Even more attention is required for the analysis and design of glass panes under exposure to fire, which is governed by a combination of multiple thermo-physical and mechanical temperature-dependent phenomena. The basic mechanical properties of materials are strongly affected by increases in temperature, and this represents a major challenge in their safe structural design. A multitude of additional aspects that play a primary role in fire endurance assessments should be taken into account, for example, geometrical and size effects, type and treatments of glass material, and the presence of further system components that are expected to interact with glass (restraints, etc.) [10]. In such an uncertain and complex context, fire endurance analyses of glass elements are hard to predict based on analytical models, instead necessitating (possibly full-scale) experiments and the integration of sophisticated Finite Element (FE) models. Fire resistance assessments of individual or assembled building components represent a fundamental requirement for construction products in the European Union according to the Construction Products Regulation (CPR) [11].

The prediction of the actual temperature field, due to either climatic actions or fire, from which thermal stresses can be evaluated, is therefore of paramount importance for designers and manufacturers of glazed elements. Besides having an eye-catching look,

these elements have to meet all load-bearing and normal functions, including those related to fire safety. Interest has also been shown by industry and public authorities worldwide, who are trying to harmonize and develop sound standards on glass elements. Considering these aspects, this paper presents an accurate review of the state of the art regarding glass elements exposed to thermal actions. First, the diverse factors influencing both climatic actions (related to time-dependent environmental temperatures and solar radiation) and fire are analysed. Then, a critical review of the analytical and numerical methods used in the literature to evaluate the temperature and stress field used for glazing, and the consequent temperature-induced state of strain and stress, the latter, which is usually referred to as *thermal stress*, is presented. Finally, a detailed overview of the current standards and codes is presented.

The objective of this research is, therefore, to evidence gaps basic assumptions and approximations of existing analytical/numerical models and standard prescriptions to address the future research for “ad hoc” design rules and reliable tools, aiming to provide a more realistic characterization of temperature and stress fields due to climatic actions or fire, considering the intrinsic sensitivity of the materials involved. This may have a high impact, especially in the development of international standards and methods of assessment, which were clearly evidenced by the stakeholders involved in the building sector.

2. Thermal Actions

2.1. The Climatic Actions

The time-dependent distribution of the temperature in a facade panel strongly depends on the thermal properties of its different components (glass, interlayers, frame, sealings, coatings, etc.) and the amount of solar radiation that is received. This is affected by the time of day, season, the panel’s inclination and orientation and, above all, the possible shadows (Figure 1a) on the panel due to adjacent buildings, trees, sunshades, fins, etc. Due to this, the various parts of the panel can be heated differently. Indeed, the shaded parts are exposed to only a portion of the solar radiation, while the glass contour is sheltered by the panel frame. The thermal problem is governed by different-in-kind heat exchange phenomena, as summarized in Figure 1b. In addition, the glass can store thermal energy according to its heat capacity. The heat exchanges that should be considered are listed in the sequel.

2.1.1. Heat Radiation

The external surface of a glazing is irradiated by the sky vault, as well as by other exterior surfaces (below the horizon), which can be treated as large enclosure surfaces [12] characterized by an atmospheric longwave irradiance R_{sky} . This can be approximated as a fraction of the blackbody emissive power, evaluated at the external environmental temperature $T_{ext}(t)$, using general variable with time. This fraction depends on the so-called effective sky emissivity ε_{sky} and is expressed as:

$$R_{sky}(t) = \varepsilon_{sky} \sigma T_{ext}^4(t) = \sigma T_{sky}^4(t), \quad (1)$$

where $\sigma = 5.67 \times 10^{-8} \text{ W}/(\text{m}^2 \text{ K}^4)$ is the Stefan–Boltzmann constant, and $T_{sky}(t)$ is the effective sky temperature. As ε_{sky} ranges from 0 to 1, the effective sky temperature is lower than the surface-level air temperature [13,14]. The sky emissivity, and consequently $T_{sky}(t)$, depend on diverse environmental parameters, such as cloudiness, relative air humidity, change in atmospheric temperature with height near the earth’s surface, and amount of water vapour in the atmosphere. Several methods have been proposed [15–17] to evaluate the sky emissivity, and an extensive review of the available empirical formula can be found in [14]. The technical literature provides a very wide range of values for $T_{sky}(t)$: according to [18], the values can range from $-43 \text{ }^\circ\text{C}$ (for cold and clear sky) to $12 \text{ }^\circ\text{C}$ (for warm and cloudy conditions), while other authors [14] record values ranging from approximately $-40 \text{ }^\circ\text{C}$ to $10 \text{ }^\circ\text{C}$ in winter and from $-30 \text{ }^\circ\text{C}$ to $30 \text{ }^\circ\text{C}$ in summer.

The radiant-energy exchange between the external (front) glass surface at a temperature $T_F(t)$ and the exterior is directly proportional to the fourth power of their temperatures, and may be written in the form:

$$q_{ext,rad}(t) = \varepsilon\sigma [T_{sky}^4(t) - T_F^4(t)]. \quad (2)$$

When the two temperatures are close one to each other (more specifically, if the temperature difference is small with respect to the mean absolute temperature, as this is usually verified for facades), Equation (2) can be approximated using the external radiation heat transfer coefficient, $h_{e,r}$, in the form [19]:

$$q_{ext,rad}(t) = h_{e,r} [T_{sky}(t) - T_F(t)]. \quad (3)$$

In addition, it is often assumed [12,20] that the internal surface of the glazing is irradiated by the internal room surfaces, which may be considered a large enclosure at the inner temperature $T_{int}(t)$ [21]. By using $T_B(t)$ to denote the temperature of the internal (back) glass surface, the radiant heat exchanged may be evaluated as:

$$q_{int,rad}(t) = \varepsilon\sigma [T_B^4(t) - T_{int}^4(t)] \cong h_{i,r} [T_B(t) - T_{int}(t)], \quad (4)$$

where $h_{i,r}$ is the internal radiation heat transfer coefficient. The values of $h_{i,r}$ and $h_{e,r}$ are prescribed by particular standards (see Section 5.2.1 and Table 1), which also furnish the external temperature, depending on the location, season, and day, while the internal temperature is usually considered constant.

2.1.2. Heat Convection

Heat convection is defined as the thermal exchange between a solid surface and an adjacent fluid at different temperatures [19]. In a glazing panel, this occurs between the “front” surface at a temperature $T_F(t)$ and the external air at temperature $T_{ext}(t)$, as well as between the “back” surface at a temperature $T_B(t)$ and the internal environment at temperature $T_{int}(t)$. Standards and codes suggest reference values for $T_{ext}(t)$ and $T_{int}(t)$ (see Section 5.2.1 and Table 2). By denoting as $h_{e,c}$ and $h_{i,c}$ the heat transfer coefficient with the external and internal environment, respectively; in this way, the heat flux may be evaluated as:

$$q_{ext,conv}(t) = h_{e,c} [T_{ext}(t) - T_F(t)], \quad (5)$$

$$q_{int,conv}(t) = h_{i,c} [T_B(t) - T_{int}(t)]. \quad (6)$$

Several empirical formulas have been proposed [22–25] to evaluate $h_{e,c}$ and $h_{i,c}$, which depend on the air velocity far from and near the surface, as well as its thermal conductivity. The latter is strongly influenced by the type of convection (natural or forced). Since, to accurately evaluate building energy performance, knowledge of the convective heat transfer coefficient distribution over the facade is important, numerical methods are employed to evaluate $h_{e,c}$, particularly for windward building facades [26–28]. However, design standards often suggest reference values for $h_{e,c}$ and $h_{i,c}$, with the former possibly being dependent on the season (see Section 5.2.1 and Table 3).

2.1.3. Solar Radiation

The radiation from the sun increases the temperature of the glass panel. Since solar radiation data are critical to the design of facades, in the past ten years, a large number of models have been developed to estimate solar radiation. A comprehensive review can be found in [29].

The total density of heat flow rate of incident solar radiation, usually denoted as $G(t)$, depends on several factors, such as the season and time of day [30,31], facade orientation

and geographic location [32–34], and panel inclination [35–37]. Several contributions to the literature have been devoted to assessments of solar radiation, both from the numerical [38–41] and the experimental [42,43] perspectives. The standards usually record values for $G(t)$ in tables and graphs as a function of the season and the facade orientation and inclination of the facade (see Section 5.2.1 and Table 4). Due to the absorption phenomena, the solar radiation is attenuated, i.e., the “available” energy decreases along the panel thickness. Using z , the through-the-thickness coordinate, with $z = 0$ at the front panel surface and $z = s$ (where s is the glass thickness) at the back surface, the absorbed energy $E(z, t)$ at the generic z increases with the distance from the external surface. According to the Bouguer–Beer–Lambert law [19,44], the absorbed energy is given by [45–47]:

$$E(z, t) = (1 - e^{-pz})G(t), \quad (7)$$

where p is the extinction coefficient of glass.

However, a convenient approximation [48] consists of assuming that the absorbed solar energy linearly increases through the layer thickness according to the glass absorptivity α , i.e.,

$$E(z, t) = \alpha G(t)z/s. \quad (8)$$

The material absorptivity α corresponds to the part that was absorbed in the whole layer, i.e., at $z = s$, so that $\alpha = (1 - e^{-ps})$ [19]. Note that the absorptivity coefficient can be modified using coatings. According to [44], this simplification is acceptable for glass layers with a standard thickness, since the crossing radiation is only weakly attenuated. This is equivalent to assuming that the solar radiation is absorbed per unit thickness, per unit time, i.e., $dE(z, t)/dz$ is constant.

2.1.4. The Influence of Shadows and Frame

The solar radiation is also affected by the presence of shadows projected on the glazing due to outside architectural features [9,34,49,50], such as mullion and transom caps, building overhang, trees [51], adjacent buildings, and shading devices. The shading is also influenced by inside parameters [52], i.e., the presence of blinds, proximity of heating appliances, and inside aeration-forcing air system. Static shadows, defined as those present for more than 3 h [53], are more critical than mobile shadows, because the former produce a cooler area of glass [9,54]. Additionally, the shadow shape influences its dangerousness, as discussed in Section 5.2.1. According to [55], it is usually assumed that the shaded parts of the glazing are hit by a portion equal to 10% of the global solar radiation.

Another important effect is the presence of the frame contouring the glass panel, totally preventing the solar radiation from hitting the glass. Obviously, the temperature of the glass edges (covered by frame) will remain at a lower temperature than that of the central area [9]. These factors lead to non-uniform temperature distribution, inducing an uneven expansion/contraction of glass within the panel and possibly leading to breakage.

According to [54,55], the presence of shadows and the contouring frame may be accounted for by defining a non-dimensional coefficient θ , multiplying the solar energy $G(t)$ and taking specific values for the different panel regions. These are as follows:

- $\theta = 1$ in glass portions directly invested by the solar radiation;
- $\theta = 0.1$ in the shaded glass portions;
- $\theta = 0$ in the framed region.

2.1.5. Heat Conduction

Heat conduction is a phenomenon occurring within the same body, or between bodies in direct contact, due to the microscopic interactions of particles [19]. When the glass panel is heated in an uneven manner, due to the presence of shadows, conductive heat exchanges take place between regions at different temperatures [56]. The heat exchange per unit is proportional to their temperature difference, the glass conductivity, and the interface area. At the plate edges, heat conduction between the glass and frame is prevented by the pres-

ence of edge seals, which usually have a very low coefficient of thermal conductivity [57], to reduce heat loss.

Note that while radiation and convection govern the out-of-plane heat flux, i.e., the heat exchange with the surrounding environment, through the front and back panel surfaces, the heat conduction is in the in-plane direction [58,59] (see Figure 1b). Since glass has a relatively low thermal conductivity, the single panel is prone to heat up and cool down in an uneven manner, resulting in an uneven temperature distribution within the panel. The diverse thermal expansion of the different panel regions can provide high tensile stresses in the cold part (usually the panel edges that are covered by the frame), leading to glass fracture [6,60] when these stresses exceed the local strength.

As discussed in Section 5.2.1, the heat conduction is usually neglected in simple analytical methods (particularly, by methods prescribed by the standards), thus inducing an overestimation of the thermal gradients. This simplified approach could result in severe/misleading estimates, especially for glass panes under fire conditions (see Section 2.2), due to the relatively high temperatures and modifications in thermo-physical and mechanical features of constituent materials as a function of temperature variations and fast increases. In this sense, both material state modifications due to high temperature and possible mutual interactions with a material brittle fracture mechanism under mechanical loads should be considered under multiple unfavourable loading combinations [61].

2.1.6. Heat Storage

The facade elements can also store thermal energy proportionally to their mass per unit volume (density) and specific heat, whose standard values are provided by codes [62], as well as to the time derivative of their temperature [19]. When the full thermal problem of glazing elements is considered, the heat fluxes from/to the surrounding environment are time-dependent, due to the daily variation in the external/internal temperatures and solar radiation, providing transient properties regarding the thermal problem.

Simplified solutions may be found by prescribing fixed environmental conditions [54]. In this case, after a certain time, the glass panel reaches a thermal equilibrium (*steady-state* condition), where the energies flowing in and out the panel become equal. In this case, no heat is stored and the temperature becomes constant over time. The time needed to reach the steady-state is strongly dependent on the heat capacity and may be evaluated by means of a “pseudo-transient” approach to the steady-state computations, accounting for the heat storage. Many simplified models (see, among others, [63–65]) neglect the heat storage, as well as the time-dependence of other contributions to heat exchange, and thus only consider the problem at the steady-state.

2.2. Fire

Fire loading, for constructional components and systems in general, represents a critical design action that can be efficiently addressed once the material response to fire exposure and the load-bearing performance under fire conditions are properly and jointly taken into account. Basically, the most efficient approach to collapse and fire endurance assessments of glass elements in fire is represented by fire tests conducted in the furnace setup. However, very few examples are available in the literature regarding material and element thermo-mechanical characterization (see, for example, [66–68]).

In terms of the characterization and description of this action, structural experiments and calculations for building components composed of traditional constructional materials assume the conventional ISO 834-1 time–temperature curve (Figure 2a).

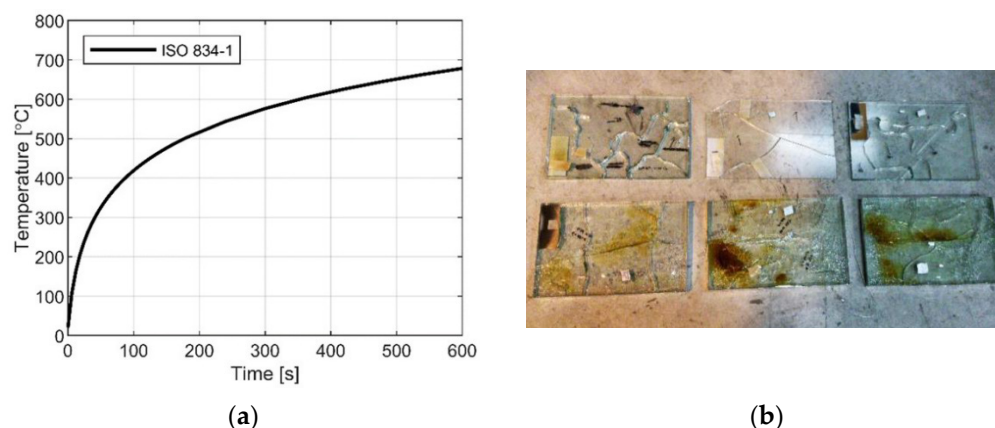


Figure 2. (a) Conventional time–temperature curve according to ISO 834-1 [69] and (b) example of non-uniform thermal exposure (after test; figure reproduced from [70] under the terms and conditions of CC-BY copyright license agreement).

Especially in recent years, the research activity on fire engineering and fire-related issues can obtain a major advantage from the efficient support of innovative methods for the realistic description of fire accidents. For example, it was reported in [61] that, for wildland–urban-level assessments of fire engineering issues, one of most frequent risks is represented by fire spreading through both wildland and urban environment, with major consequences for constructed facilities and, especially, glazed building enclosures. As such, the main input used data to evaluate the fire event are the building’s use, the room geometry, the available fuel and the wall insulation, as well as the presence of ventilation systems.

In this regard, while it is rationally accepted that the temperature evolution in Figure 2a can also be efficiently applied to load-bearing elements made of monolithic or laminated glass, a major uncertainty can derive from engineering knowledge and the characterization of intrinsic material properties, especially in terms of radiation and convection interactions for the exposed and unexposed glass element surfaces and the surrounding air [70]. Further uncertainty can derive from the description of restraints (for example, in the framed system of Figure 1a) and their consequences for the local/global performance of glass components (see Figure 2b and [71]). For vertical glass elements such as windows and walls, a major uncertainty in analysis and modelling is represented by the actual non-uniform thermal exposure on the elevation, and its consequences for load-bearing performance considerations [72,73]. However, the few experimental validations of detailed numerical models suggest the rather high potential and reliability of simulations for the interpretation and extension of experiments in the furnace setup.

3. The Determination of the Temperature Field in Glazing

The scientific and technical literature contain several studies analyzing the heat exchange phenomena in fenestrations subjected to climatic actions. However, they are mainly devoted to the evaluation of the overall thermal transmittance (U-value) of the glazing element (see, among others, [74–78]). However, a precise evaluation of the temperature field of the glazing is required when one is interested in the assessment of thermally induced stress.

Few research studies can be found in the literature focusing on fire-loading, and the fire endurance of ordinary soda-lime glass with a load-bearing role in buildings is still an open challenge, with potential safety risks [67]. Regarding the standardized regulations for load-bearing, building elements composed of more traditional construction materials are considered, and the progressive temperature propagation and increase in the glass surface and thickness represent the primary engineering goals of experiments and numerical simulations. However, experimental studies are still rather limited in the literature, and numerical methods still suffer for uncertainties, as they are robust but have limited validation to few structural experiments under fire conditions.

3.1. The Governing Equations and Boundary Conditions

3.1.1. Monolithic Glass

The thermal problem of a glazing panel is governed by the traditional three-dimensional heat equation [19]. By denoting the in-plane directions using (x, y) , and the through-the-thickness coordinate using z , this may be written as:

$$\rho c_p \frac{\partial T(x, y, z, t)}{\partial t} = \lambda \left[\frac{\partial^2 T(x, y, z, t)}{\partial x^2} + \frac{\partial^2 T(x, y, z, t)}{\partial y^2} + \frac{\partial^2 T(x, y, z, t)}{\partial z^2} \right] + \frac{\partial E(z, t)}{\partial z}, \quad (9)$$

where ρ denotes the mass per unit volume of glass, c_p is the specific heat, and λ is the thermal conductivity. In words, this is equivalent to requiring that the heat stored in the glazing in the unit time per unit volume (represented by the l.h.s. of Equation (9)), is equal to the sum of the heat transmitted by conduction and the contribution of solar radiation $E(z, t)$ (see Equations (7) and (8)).

If the steady-state problem is considered, the heat storage contribution can be neglected, and the temperature field becomes independent of the time variable. The boundary conditions for the front surface ($z = 0$), which is in contact with the external environment, and the back ($z = s$) surface, which is in contact with the inner one, respectively, are:

$$\begin{aligned} -\lambda \left. \frac{\partial T(x, y, z, t)}{\partial z} \right|_{z=0} &= q_{ext}(t), \\ -\lambda \left. \frac{\partial T(x, y, z, t)}{\partial z} \right|_{z=s} &= q_{int}(t), \end{aligned} \quad (10)$$

where, when climatic actions are considered, the considered surface fluxes are those given by Equations (3)–(6), and:

$$\begin{aligned} q_{ext}(t) &= q_{ext,conv}(t) + q_{ext,rad}(t), \\ q_{int}(t) &= q_{int,conv}(t) + q_{int,rad}(t). \end{aligned} \quad (11)$$

At the plate edges, it may be required that the in-plane heat flux is nil [79].

Simplified models [70,79] aiming to evaluate the “centre glass” temperature, that is approximately independent of the in-plane coordinates, consider the one-dimensional (1D) version of the heat conduction in Equation (9), i.e.,

$$\rho c_p \frac{\partial T(z, t)}{\partial t} = \lambda \frac{\partial^2 T(z, t)}{\partial z^2} + \frac{\partial E(z, t)}{\partial z}. \quad (12)$$

In this case, only out-of-plane boundary conditions (10) are needed.

Approximated models have also been proposed in the literature, where the solar radiation is modelled as a heat source in correspondence with the external surface. This simplifying assumption leads to a linear distribution of the temperature in the through-the-thickness direction, providing a null, thermally induced stress [79,80]. This will be discussed more in detail in Section 4.1.

For glazing under fire in both the monolithic and laminated configurations, similar assumptions are made. Various studies of the literature, however, show that simplified 1D modelling assumptions are only accurate for very simple calculations (Figure 3) and are not able to capture the spatial and temporal evolution of thermo-mechanical phenomena.

3.1.2. Laminated Glass

When considering laminated glass composed of glass plies bonded by polymeric interlayers and/or glass with coatings [81–83], the thermal problem is complicated by the presence of different layers with different thermal conductivities λ and different specific heat per unit volume ρc_p [47,70,79,84]. In this case, the heat-conduction Equation (9) (or Equation (11) if the 1D problem is considered) holds for each of the plies comprising the glazing, while proper interface conditions (i.e., the continuity of the temperature field and of the heat flux) should be required [70,79]. By considering the generic i -th and j -th plies,

with an interface located at $z = \bar{z}$, the interface conditions that must be satisfied $\forall(x, y, t)$ are [79,84]:

$$\begin{aligned} T_i(x, y, z, t) \Big|_{z=\bar{z}} &= T_j(x, y, z, t) \Big|_{z=\bar{z}}, \\ \lambda_i \frac{\partial T_i(x, y, z, t)}{\partial z} \Big|_{z=\bar{z}} &= \lambda_j \frac{\partial T_j(x, y, z, t)}{\partial z} \Big|_{z=\bar{z}}. \end{aligned} \quad (13)$$

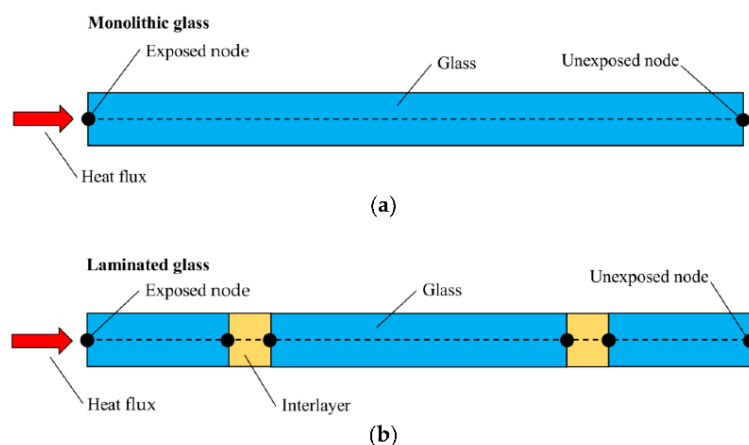


Figure 3. Schematic representation of a reference 1D heat transfer model for (a) monolithic and (b) laminated glass elements (cross-section layout). Figure reproduced from [70] under the terms and conditions of the CC-BY copyright license agreement.

The second row of Equation (13) implies that, at the interfaces, the spatial derivatives of the glass and interlayer temperatures are not equal, being inversely proportional to the ratio of the thermal conductivities of the two materials. The precise calculation of the temperature at each point as a function of time hence requires a three-dimensional analysis [19,80].

3.1.3. Insulating Glass Units

Insulating glass units (IGUs) are formed of two or more glass panes held together by structural edge seals, entrapping gas for thermal and acoustic insulation. A commonly used, practical way to decrease the thermal losses and improve the acoustic performance is to increase the number of gas-filled gaps: this is why multiple panes composing IGUs are widely used in the building industry at present. The load-bearing capacity of these elements is enhanced by the coupling of the panes [85,86] via the internal pressure of the gas, resulting in so-called *load-sharing* [87–89].

The thermal problem of IGUs must be treated with particular care. Indeed, in addition to the heat exchanges considered in Section 2.1, the heat exchange between the different panes, as well as the gas filling the cavities, must be considered. Two main phenomena have to be considered:

- Heat convection occurs at the external surface, between the “front” panel and the external air, as well as at the internal surface between the “rear” panel and the indoors, and between each panel and the gas occupying the adjacent cavities. The internal convective heat transfer coefficients depend on the gas type and the cavity thickness [90–93]. The presence of the spacers usually prevents heat exchange in the edge region; hence, the heat flux at the periphery surfaces of the cavity is null [94]. Note that this implies that the (time-dependent) gas temperature is an additional variable of the thermal problem, which remains to be determined [8,55,79].
- When the radiant energy from the sun and surrounding environment strikes the front and rear glass pane, a part of the energy is absorbed by the material, a part is reflected, and the remaining part is transmitted according to the glass’ absorptivity, reflectivity and transmissivity. Hence, a fraction of the energy is transmitted to the inner panes and will be further split in three parts. This leads to multiple reflections between the glass panes

comprising the IGUs, as schematically indicated in Figure 4. Several methods have been proposed to evaluate this multiple-reflection phenomenon [48,91,95,96], with the aim of calculating the effective thermal properties (transmittance and insulation) of multiple glazing. The system of equations governing the problem is usually solved by numerical methods [48,97–100], but there are simple cases in which the solution can be analytically determined [55,56].

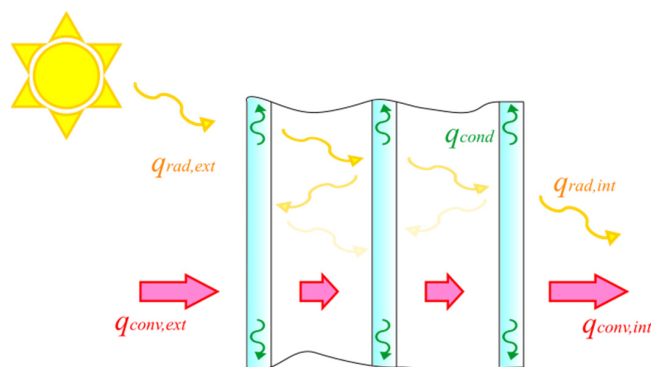


Figure 4. Schematics of the heat exchange phenomena occurring in an IGU.

For ventilated and double-skin facades, the problem is even more complicated [101–104].

Another important phenomenon that should be considered for IGUs is that temperature variations in the gas filling the cavities results in a variation in gas pressure, causing internal actions that have effects on all the panes [85,105–107].

3.2. Analytical and Numerical Solutions for Glazing under Climatic Actions

The models proposed by the literature, as well as by standards (that will be discussed in more detail in Section 5) are usually based on simplifying assumptions. In the design practice, one of the main simplifications adopted for monolithic panes and panes composing IGUs is that the temperature profile is uniform in the thickness direction. This corresponds with assumptions that the pane is *thermally thin* [108,109], i.e., the temperature variation through the panel thickness is negligible with respect to the temperature variation at the surfaces due to convective heat exchange. This assumption is acceptable for monolithic glass of standard thickness, of the order of 1 cm. More refined approaches [48] consider two different temperatures at the back and front surfaces, which can be evaluated by assuming that the solar energy is uniformly absorbed through the thickness.

The analytical solutions available in the literature can be divided into two main categories:

- 1D models, aiming to determine the temperature profile across the pane that is supposed to be independent of the in-plane coordinates [44,45,48,79,84].
- Three-dimensional (3D) models, accounting for the non-uniform heating in the different panel regions [54,55]. These models assume that the glass plate is thermally thin, hence providing a uniform temperature throughout the thickness.

In recent years, many numerical approaches have been proposed to assess the temperature field in non-uniformly heated glazing. These can be substantially classified as follows:

- Simple 1D and two-dimensional (2D) models, which can be solved by implementing governing equations with finite difference methods [46,47,70,79,110].
- 3D approaches relying on FE software solutions. These are mainly used for complex geometries, such as laminated glass elements [72,73,111] and IGUs [8], and may be coupled with the assessment of thermal stresses.

The temperature distribution of glass and facade components [6,112] may be also evaluated by means of dedicated software, also allowing for the study of complex geometries, such as IGUs and double-skin facades.

However, they are mainly devoted to determining the U-values (thermal transmittances) of windows and curtain walls. Other numerical formulations [113–115], specifically conceived for the analysis of non-uniformly heated plates, are recorded in the literature. Recently, a dedicated semi-analytical model, based on Biot’s variational principle, has been proposed [58] to evaluate the temperature field in monolithic glazing under uneven climatic action, accounting for the presence of shadows and frame. The examples presented in [59] show that the width of the transition zone is ten times the thickness of the glass, whereas the temperature profile can be approximated by a sigmoid curve. However, it has to be noted that, as stated by [116], there is a lack of uniformly defined procedures for the calculation (stationary or transient, considering the time period, etc.) and assumptions for the simulation parameters.

3.3. Numerical Solutions for Glazing under Fire

Specific numerical formulations are also available, such as that proposed by Jeffers and collaborators [113–115], which considers a combination of FE and control volume techniques for the thermal analysis of non-uniformly heated shell structures, allowing for evaluations of the temperature field due to fire action. In more detail, this approach is based on a shell heat-transfer element, but requires a very fine discretization of the panel in the thickness direction.

Several applications for the thermo-mechanical analysis of glass elements under fire exposure can be found in [66,67,70]. Uncoupled thermal and mechanical simulation steps were developed to track the temperature evolution over time, and successively account for material modifications, as in Section 4.2.1. In this manner, the cited literature contributions show that the performance of the glass following exposure to fire can efficiently reproduce the experimental observations on small- or full-size specimens, both for monolithic and laminated glass. To this aim, the most important modelling and calibration steps shown in Figure 5 can be adopted.

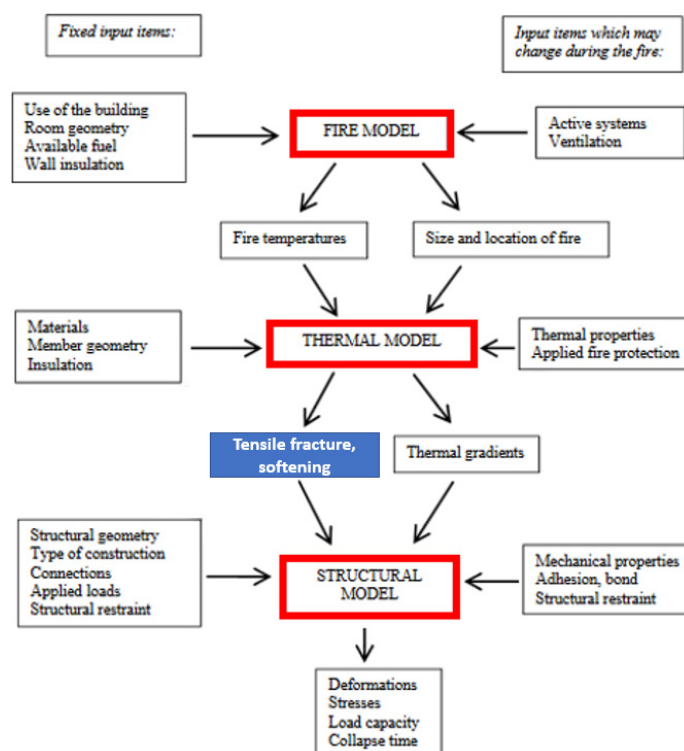


Figure 5. Procedural steps for thermo-mechanical numerical analysis of load-bearing components and structures under fire conditions (reproduced from [61] under the terms and permission of a CC-BY copyright license agreement).

4. The Thermal Stress

The determination of the 3D time-dependent temperature distribution of the glazing, as detailed in Section 3, is the starting point for a proper evaluation of the consequent temperature-induced state of strain and stress. Thermal strains are strains that develop when a material is heated or cooled with respect to a reference temperature T_0 . By using α_T to denote the coefficient of thermal expansion, the thermal strain tensor is given by:

$$\varepsilon_T(x, y, z, t) = \alpha_T [T(x, y, z, t) - T_0] I \quad (14)$$

where I is the identity 3×3 tensor. The stress tensor is given by:

$$\sigma(x, y, z, t) = C[\varepsilon(x, y, z, t) - \varepsilon_T(x, y, z, t)] \quad (15)$$

where C is the constitutive elastic tensor and $\varepsilon(x, y, z, t)$ is the total strain tensor, accounting for both the thermal and the mechanical parts of the deformation, a priori unknown, that must satisfy the compatibility relations.

When the tensile thermal stresses exceed the local strength of the glass, the panel may break. An analysis of existing cases has evidenced that most failures are due to the stresses caused by climatic actions [5], as shown by Figure 6.

Many cases of damage can be attributed to the uneven temperature distribution in the glass panes due to the presence of frame and shadows. In these cases, a so-called “thermally induced fracture” takes place, sometimes as a result of large in-plane temperature differences within the glass [6,8]. This kind of crack usually develops from the panel edge, as shown in Figure 6, which usually presents with a lower strength than the panel surface [117–120].



Figure 6. Example of glass panes with cracks due to climatic-induced thermal shock (figures reproduced from [60,121] with permission from Elsevier©, copyright license agreement n. 5507161319840, March 2023).

In cases of fire loading, totally different thermo-physical and mechanical phenomena can jointly take place in very short time intervals. Most importantly, as shown in Figure 7, softening of glass material generally prevails on the typical brittle in tension fragility.

4.1. Climatic Actions

Although temperature differences due to environmental actions are generally mild, they are often referred to as *thermal shock*, a term that is somewhat abused since it evokes strong thermal gradients, but which confirms the criticality of the phenomenon. For climatic loads, causing temperature variations of the order of 10–20 °C in the glass panes [54], the mechanical properties and temperature field are not influenced by each other. The thermal stress may be found by considering an *uncoupled* thermo-elastic problem [122,123] where the determination of the temperature field is independent of that of the stress and strain fields, while the stress and strain fields (which are dependent on the temperature distribution) may be determined a posteriori by considering the thermal strain as an applied action that varies over time.



Figure 7. Example of collapse configuration for glass under fire: (a) triple-laminated glass beam in bending setup (figure reproduced from [67] with permission from Elsevier©, copyright license agreement n. 5507161319839, March 2023) and (b) details of glass softening in the frame region.

In [60], an analytical solution to the stress field is provided for the simple cases of (i) an axi-symmetric variable temperature profile, i.e., a temperature that changes from one radial location to another with respect to a pole, and (ii) an axial-symmetric variable temperature profile with an axis of symmetry that is parallel to two sides of a square panel. In both cases, the temperature profile is considered uniform regarding the glass thickness.

For simple cases (for example, for the 1D case, where the temperature field is uniform in the in-plane directions), it is possible to find an analytic solution by following the procedure pointed out in [80], consisting of two phases. First, the plate is considered as in-plane constrained at its borders, and the external constrain reactions, which provide a homogenous stress state in the in-plane directions, are evaluated. Secondly, the stress state in the free pane is evaluated by superposing this stress field to that due to the constrain reaction, with the opposite sign (to simulate the “removal” of the constraints). When the 1D problem is considered by assuming a uniform, or linearly varying, temperature profile in-the-thickness, this results in a null stress state. This is because the temperature field produces a compatible thermal strain, which does not give raise to thermal-induced eigenstresses in an isolated plate [80]. In this case, the thermal strain tensor $\varepsilon_T(x, y, z, t)$ of Equation (13) fulfils the compatibility relations; hence, both equilibrium and compatibility are satisfied when the plate is in a stress-free state [79].

Remarkably, this means that most of the methods currently proposed by the standards and literature [12,55] and adopted in the design practice that rely on this kind of simplifying assumption, as discussed in Section 5.2.2, do not allow for the proper estimation of thermal stress. As discussed in Section 5.2.3, current codes usually provide very simple formulae, based on empirical coefficients, to evaluate the maximum stress due to thermal loads. Recently, a 3D numerical model has been proposed for the evaluation of thermally induced stress during architectural monolithic glazing under uneven conditions [124].

For laminated and layered glazing elements, and even more when coatings are used, this problem is complicated by the complex temperature distribution across the thickness, as well as by the temperature-dependent mechanical properties of the polymers used as interlayers [125–127]. Furthermore, in this case, the layer-wise mismatch of thermal and elastic properties can induce stress concentrations at the interfaces [128,129]. The different mechanical properties of glass and polymeric foils should be accounted for by considering that the interlayers are much thinner and more compliant than glass and, hence, cannot present flexural stiffness per se [130,131]. This can be accounted for in numerical analyses by considering that the polymer impedes the slippage between glass layers, which bend in parallel, by transferring shear stress. The shear stress of the interlayer breaches the principle of “straight normal remaining straight after deformation”, on which the conventional shell elements of FE analysis are based. Hence, the modelling of the thermo-elastic problem deserves particular attention [132].

In conclusion, numerical modelling is often used only to predict the thermal stresses once the temperature field is known. The numerical approaches proposed by the literature [133] are mainly devoted to the study of glazing under fire, and will be discussed in Section 4.2. However, these can also be used to evaluate climatic-induced stress. Let us note that, for the latter case, the key point is to determine the actual temperature distribution in glass since, if this is uncertain, the numerically evaluated stresses are of no practical interest.

4.2. Fire

The fire performance and endurance assessment of glass elements, based on numerical tools, is one of the major open issues for the design and maintenance of ordinary glass components in buildings at present. The major challenges derive, as discussed above, from the lack of certain performance indicators to address the fire endurance [134], but also from basic uncertainties in the fire loading, fire exposure and fire sensitivity of material properties.

4.2.1. Material Properties in Fire

In fire conditions, a major challenge is represented by the structural design and optimization of load-bearing or secondary components, which are composed of materials with high sensitivity to temperature. According to the literature, few experimental investigations are available for the characterization of glass under fire conditions. In addition, the scientific community agrees with the typical material properties reported in Figure 8, where variations can be tracked up to a minimum of 600 °C. Most importantly, the modulus of elasticity of glass under high temperatures suffers from high degradation due to progressive melting and the solid-state modification of glass material. From a structural perspective, such behaviour suggests that major modifications can be expected to the strain-stress performance and capacity to sustain ordinary loads.

4.2.2. Numerical Solutions

The thermo-mechanical performance assessment of structural elements exposed to fire is typically modelled by a series of uncoupled (or even sequentially coupled) analyses, following the procedure outlined in Figure 5. In the first stage, a thermal simulation (heat transfer analysis) is carried out to evaluate the temperature distribution and propagation in time (including the accurate description and characterization of thermal restraints). Nodal temperatures at each time increment represent a key output of analysis. Successively, a mechanical analysis is carried out to assess the structural response of the system, by considering any external action but especially the modification of material properties with temperature, and thermal corresponding expansion [61,113,135,136].

Generally speaking, the current literature suffers from the limited number and applications of experimental tests on the effects of fire on glass elements, which could be variably loaded and restrained, as in real buildings. As a matter of fact, the available numerical studies are thus necessarily elaborated on specific configurations of technical interest ([66,67], etc.). While the current research advancements in this direction are still weak in terms of the generalization of numerical outcomes and definition of standardized procedural steps for fire endurance assessments of variably loaded and restrained glass elements [134], the potential of these first efforts and contributions is represented by the univocal description and calibration of basic material properties (see Figure 8), thermal interactions at the exposed and unexposed surfaces, and the fire loading schematization.

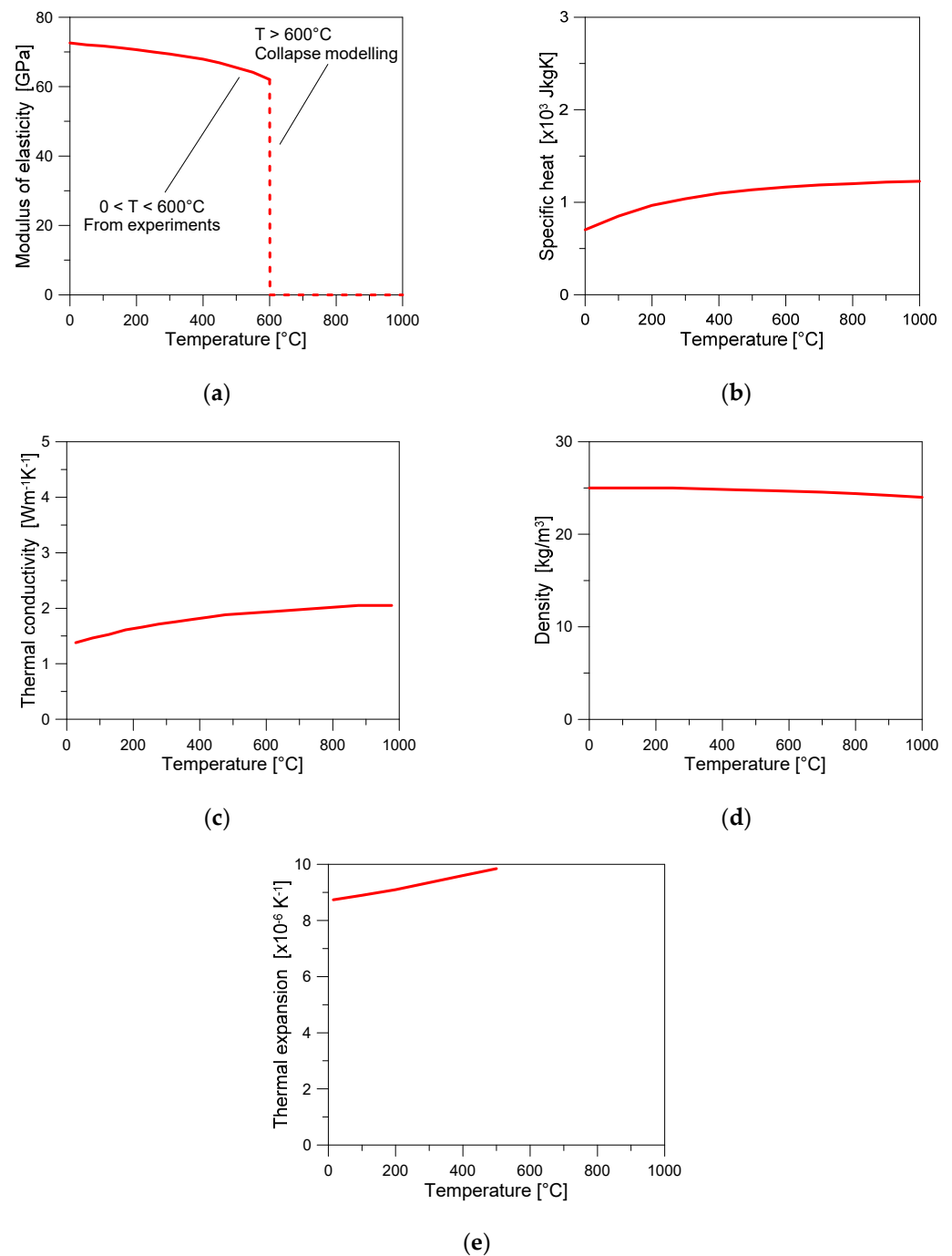


Figure 8. Selected glass material properties for ordinary soda-lime annealed glass, with evidence of their sensitivity to temperature variations: (a) modulus of elasticity; (b) specific heat; (c) thermal conductivity; (d) density; (e) thermal expansion coefficient (figure adapted from [136] under the terms and conditions of a CC-BY copyright license agreement).

5. Standards and Codes

5.1. Physical and Mechanical Properties of Glass and Glazing Components

For the proper design of glazing components, especially when dealing with their thermal performance, knowledge of the current standards providing methods and tests for the evaluation of glass' mechanical and thermal properties becomes necessary. EN 572-9 [137] is the harmonized standard that is necessary for the CE marking of glass products and provides the general physical and mechanical properties of glass. EN 572 is composed of nine parts, the

first one of which [62] specifies and classifies the basic glass products, their main properties and the general quality criteria.

A calculation method regarding the thermal resistance and thermal transmittance of building components and building elements is provided in EN ISO 6946 [20]. This calculation method uses the “design thermal conductivities” or, equivalently, the “design thermal resistances”, of the materials and products appropriate for the considered application. The components and elements to which the method can be applied should consist of thermally homogeneous layers (which can include air layers). Specific aspects related to glazing are instead contained in EN 673 [138], which details a calculation method to determine the U-value, a measure of the rate of heat transfer through a structure, of glazing. This provides not only the basic formulas, but also the basic material properties of both glass and gas filling the gaps in double glazing, as well as of the external and internal heat transfer coefficients. When talking about glazing components and their thermal performances, the particular role of the frame should be highlighted. Therefore, EN ISO 10077-2 [139] provides a calculation method for the thermal transmittance of frame profiles and their relative connections with glass or opaque panels. The method can also be used to assess the thermal resistance and thermal characteristics of shutter profiles or roller shutter boxes and similar components (e.g., blinds). EN 410 [140] and ISO 9050 [141] are mainly focused on optical and solar glazing properties, which are necessary aspects for lighting, heating and cooling calculations in buildings. EN 12898 [142], which specifies a procedure for determining the emissivity (at room temperature) of the glass and coated glass surfaces, should also be mentioned. This is a necessary step to consider heat transfer by surfaces radiation to determine the U-value and of the total solar transmittance of glazing. Finally, ISO 15099 [12] details calculation techniques for determining the thermal and optical transmission characteristics (i.e., thermal transmittance and total solar energy transmittance) of window and door systems, including the relevant solar and thermal properties of all components, while EN ISO 52022 [143,144] specifies either simplified or detailed methods based on the solar and light properties of protection devices combined with glazing to determine the relevant solar-optical information of the combination of these components (such as the total solar energy transmittance and total light transmittance).

In terms of the glass design, standards or guidelines that also consider the thermal stresses due to climatic actions include the Italian Guidelines [121], the three parts of the new European CEN/TS 19100 [145–147] and the French standard [55]. Some instructions for the calculation of the thermal stresses are given in the Belgian Guidelines [148], the Pilkington Instructions [149], mostly used in the UK, and the European standard [150], which is currently just a proposal and not an officially accepted standard.

In the following paragraphs, reference will be made to each of these standards and codes in order to provide information on how the different coefficients and calculation methods are dealt with in the available few references.

5.2. Climatic Actions

5.2.1. Heat-Exchange Contributions

As seen in Section 2.1, the governing equations of the thermal problem are derived from the analysis of the different heat-exchange phenomena. It is therefore useful to summarize how the different contributions are dealt with in the various standards (see also Tables 1–4).

Heat radiation

As stated in Section 2.1.1, $h_{i,r}$ is the internal radiation heat transfer coefficient, while $h_{e,r}$, the external radiation heat transfer coefficient. The values of $h_{i,r}$ and $h_{e,r}$ are generally prescribed by standards. EN ISO 6946 [20] furnishes values of these coefficients in tables for a glass emissivity of $\varepsilon = 0.9$ ($h_{i,r} = 4.59 \text{ W}/(\text{m}^2\text{K})$ and $h_{e,r} = 5.13 \text{ W}/(\text{m}^2\text{K})$). EN 673 [138] provides the value for the internal radiation heat transfer coefficient ($h_{i,r} = 4.1 \text{ W}/(\text{m}^2\text{K})$), but the value of the external coefficient is not given. The French standard [55] refers to

EN 673 for such coefficients in the case of IGU, while ISO 15099 [12] provides closed-form equations (Table 1).

Table 1. Heat radiation contributions according to different standards.

HEAT RADIATION		
	$h_{i,r}$	$h_{e,r}$
CNR DT 210	-	-
EN ISO 6946	4.59 W/(m ² K) (Table 5)	5.13 W/(m ² K) (Table 5)
EN 673	4.1 W/(m ² K) <i>Vertical (uncoated) soda lime glass surfaces</i>	-
EN ISO 10077-1	-	-
DTU 39	acc. to EN 673 <i>(only for IGU)</i>	-
ISO 15099	$h_{r,in} = \frac{\epsilon_{s,in}\sigma(T_{s,in}^4 - T_{rm,in}^4)}{T_{s,in} - T_{rm,in}}$	$h_{r,ex} = \frac{\epsilon_{s,ex}\sigma(T_{s,ex}^4 - T_{rm,ex}^4)}{T_{s,ex} - T_{rm,ex}}$
EN 52022-3	-	-
BELGIAN GUIDELINES	-	-
PILKINGTON INSTRUCTIONS	-	-

Heat convection

Convection heat transfer is the energy transfer between a surface and a moving fluid. Therefore, it depends on the temperature of the moving fluid (i.e., air, internal or external) and that of the window surface (see Section 2.1.2). Many standards suggest reference values for $T_{ext}(t)$ and $T_{int}(t)$, the latter usually assumed to be constant, see Table 2.

In the absence of specific information for the building under consideration, CNR DT 210 [121] refers to UNI 5364 [151], which summarizes in tables the conventional internal air temperatures as a function of various standardized internal areas. The external air temperature is obtained by reference to maximum and minimum values, defined as maximum summer and minimum winter air temperature, respectively, in the location of the building, considering a 50-year return period. One may assume a temperature variation between the extreme values $\Delta T = \pm 30$ °C. The French standard [55] gives different values when considering the transient or the steady-state regime. In the former case, the maximum and minimum values of the external temperature are indicated in maps for France; in the latter case, values are given in tables as a function of the season. The internal temperature of the area of the buildings in service is assumed to be constant and is given in Table 5 of the standard. ISO 15099 [12] furnishes reference boundary conditions among which constant values of T_{int} and T_{ext} are given for summer and winter conditions (T_{int} ranging from 20 °C to 25 °C and T_{ext} from 0 °C to 30 °C, respectively). The same values of T_{int} are given by EN 52022-3 [144], while T_{ext} has slightly different values (from 5 °C to 25 °C). A diurnal temperature range is given from graphs as a function of the location in the Pilkington Instructions [149]; however, this cannot be considered a standard and seems to only be valid for the Pilkington glasses. The Belgian Guidelines [148] only provide the maximum amplitude of the average diurnal temperature fluctuations over at least 10 years in the different provinces of Belgium.

Table 2. Heat convection contributions according to different standards.

Heat Convection				
	T_{ext}	T_{int}	$h_{i,c}$	$h_{e,c}$
CNR DT 210	Max summer and min winter air T (50 y return period). Initial assumption $\Delta T = \pm 30$ °C between extreme values.	Tables f (standardized internal areas) (UNI 5364)	-	-
EN ISO 6946	-	-	3.6 W/(m ² K) (for free convection)	-
EN 673	-	-	-	-
EN ISO 10077-1	-	-	-	-
DTU 39 ⁽¹⁾	TR: Table 4 for each season f (max and min diurnal T and amplitude) (France only) SS: Winter: min diurnal T (France maps) + 5 °C	Constant value f (facade inclination and season) (Table 5)	acc. to EN 673 (only for IGU)	-
ISO 15099	Reference BC (§8.2) Win: 0 °C Sum: 30 °C	Reference BC (§8.2) Win: 20 °C Sum: 25 °C	<ul style="list-style-type: none"> ■ Nu (λ/H) ⁽²⁾ (natural convection) ■ $4 + 4v$ ⁽²⁾ (forced air flow for product comparison) or $4.7 + 7.6v$ (forced air flow in real buildings)- if surface windward ⁽³⁾: $v = 0.25V$ for $V > 2$ m/s $v = 0.5V$ for $V \leq 2$ m/s - if surface leeward ⁽³⁾: $v = 0.3 + 0.05V$ 	<ul style="list-style-type: none"> ■ Nu (λ/H) ⁽²⁾ (natural convection) ■ $4 + 4v$ ⁽²⁾ (forced air flow) [from EN ISO 6946]
			Reference BC (§8.2) Winter: 3.6 W/(m ² K) Summer: 2.5 W/(m ² K)	Reference BC (§8.2) Winter: 20 W/(m ² K) [4 m/s] Summer: 8 W/(m ² K) [2 m/s]
EN 52022-3	Reference BC (§6.4.6) 5 °C Summer (§6.4.6) 25 °C	Reference BC (§6.4.6) 20 °C Summer (§6.4.6) 25 °C	Reference BC (§6.4.6) 3.6 W/(m ² K) Summer (§6.4.6) 2.5 W/(m ² K)	Reference BC (§6.4.6) 18 W/(m ² K) Summer (§6.4.6) 8 W/(m ² K) (for $v = 1$ m/s)
BELGIAN GUIDELINES	-	-	-	-
PILKINGTON INSTRUCTIONS	-	-	-	-

⁽¹⁾ SS: Steady state; TR: Transient regime; ⁽²⁾ Nu Nusselt number, λ air thermal conductivity, v free stream velocity adjacent to the surface, m/s; ⁽³⁾ V wind velocity (H = 10 m above ground level).

Regarding the convective heat transfer coefficients, EN ISO 6946 (Table C.1) furnishes the following values: $h_{i,c} = 5$ W/(m²K) for upward heat flow; 2.5 W/(m²K) for horizontal heat flow and 0.7 W/(m²K) for downward heat flow. The external values are given by $h_{e,c} = 4 + 4v$, where v is the wind speed adjacent to the surface, in m/s (the same value is also recalled by ISO 15099 in case of forced convection). For a speed of 4 m/s (see Note 2 in Table 7 of EN ISO 6946), this coefficient becomes 20 W/(m²K), as also reported in Table 5 of the same standard.

EN 673 [138], which is specific to glass and to which the French standard also refers, does not provide values for the external convective contribution, but it provides standard

values for the internal coefficients for vertical (uncoated) soda lime glass surfaces and free convection: $h_{i,c} = 3.6 \text{ W}/(\text{m}^2\text{K})$.

ISO 15099 (and also EN 52022-3) also distinguishes between winter and summer conditions for the convective heat transfer coefficients: ($h_{i,c} = 3.6 \text{ W}/(\text{m}^2\text{K})$ and $h_{e,c} = 20 \text{ W}/(\text{m}^2\text{K})$ in winter conditions and $h_{i,c} = 2.5 \text{ W}/(\text{m}^2\text{K})$ and $h_{e,c} = 8 \text{ W}/(\text{m}^2\text{K})$ for summer conditions). However, more refined assessments are presented for the convective heat transfer coefficients on the internal and external side of the glazing system, which also function to assess the type of convection (natural or forced air flow), see Table 2.

Surface exchange coefficients (convection + radiation)

According to EN ISO 6946 [20], an operative temperature (usually approximated to the arithmetic mean of air temperature and mean radiant temperature) is generally taken to calculate the heat flow rates for the environment inside the buildings, while “at external surfaces it is conventional to use the external air temperature, based on an assumption of overcast sky conditions, so that external air and radiant temperatures T_{ext} and T_{sky} are effectively equal” (see EN ISO 6946, footnote 3). Therefore, total combined heat transfer coefficients $h_i = h_{i,c} + h_{i,r}$ and $h_e = h_{e,c} + h_{e,r}$ are defined, to account for both the heat convection contribution (Section 2.1.2) and that from infrared radiation (sky radiation and indoor radiation, Section 2.1.3), in the unique formula:

$$q_{ext}(t) = q_{ext,conv}(t) + q_{ext,rad}(t) = h_e [T_{ext}(t) - T_F(t)], \quad (16)$$

$$q_{int}(t) = q_{int,conv}(t) + q_{int,rad}(t) = h_i [T_B(t) - T_{int}(t)]. \quad (17)$$

It may be observed that this approximation prevents the consideration of different values for $T_{ext}(t)$ and $T_{sky}(t)$; therefore, it neglects the influence of atmospheric temperature, the clarity of the sky and humidity.

Considering this approach, a few standards directly prescribe values for the internal and external surface exchange coefficients.

EN ISO 6946 [20] prescribes the following values for the “conventional surface resistances” (correspondent to the reciprocal of heat transfer coefficient): for the inner surface, $0.1 \text{ m}^2\text{K}/\text{W}$, $0.13 \text{ m}^2\text{K}/\text{W}$ and $0.17 \text{ m}^2\text{K}/\text{W}$ for upwards, horizontal and downwards heat flow, respectively; for the outer surface, $0.04 \text{ m}^2\text{K}/\text{W}$. These correspond to the following total surface heat transfer coefficient values: $h_i = 10 \text{ W}/(\text{m}^2\text{K})$ for upward heat flow, $7.7 \text{ W}/(\text{m}^2\text{K})$ and $5.8 \text{ W}/(\text{m}^2\text{K})$ for horizontal and downwards heat flows and $h_e = 25 \text{ W}/(\text{m}^2\text{K})$. Such values are also suggested by EN ISO 10077-1 (Table E.1) [152] and recorded by the Italian CNR DT 210 (Table 4.16) [121]. EN 673 [138], which is specific to glass, furnishes the same value for the total external surface heat transfer coefficient ($h_e = 25 \text{ W}/(\text{m}^2\text{K})$), without giving information on the convective and the radiative contributions. Furthermore, standard values are provided for the internal coefficients for vertical (uncoated) soda lime glass surfaces and free convection: $h_{i,c} = 3.6 \text{ W}/(\text{m}^2\text{K})$ and $h_{i,r} = 4.1 \text{ W}/(\text{m}^2\text{K})$, leading to $h_i = 7.7 \text{ W}/(\text{m}^2\text{K})$. The French standard [55] reports different values for vertical or inclined surfaces and differentiates the external coefficient as also being a function of the season. For vertical surfaces, $h_i = 9 \text{ W}/(\text{m}^2\text{K})$ and $h_e = 11 \text{ W}/(\text{m}^2\text{K})$ in winter and mid-seasons, and $h_e = 13 \text{ W}/(\text{m}^2\text{K})$ in summer. The Belgian Guidelines [148] directly furnish an internal surface exchange coefficient of $h_i = 8 \text{ W}/(\text{m}^2\text{K})$ and an external one of $h_e = 11 \text{ W}/(\text{m}^2\text{K})$.

In summary, most standards provide a value of $h_i = 7.7 \text{ W}/(\text{m}^2\text{K})$ for vertical surfaces (horizontal heat flow), with slight differences provided by the French standard and the Belgian Guidelines ($h_i = 9 \text{ W}/(\text{m}^2\text{K})$ and $h_i = 8 \text{ W}/(\text{m}^2\text{K})$, respectively). A similar situation occurs for the external exchange coefficient, which is generally provided as $h_e = 25 \text{ W}/(\text{m}^2\text{K})$. However, both the French and Belgian instructions provide much lower values, which are equal to $11 \text{ W}/(\text{m}^2\text{K})$ and $16 \text{ W}/(\text{m}^2\text{K})$, respectively. For direct comparison, a summary of these values is reported in Table 3.

Table 3. Surface exchange coefficients according to different standards.

SURFACE EXCHANGE COEFFICIENTS (CONVECTION + RADIATION)				
	h_i		h_e	
	Vertical	Horizontal (Or Inclined)	Vertical	Horizontal (Or Inclined)
CNR DT 210	7.7 W/(m ² K) [1/h _i = 0.13 m ² K/W]	10 W/(m ² K) [1/h _i = 0.1 m ² K/W]	25 W/(m ² K) [1/h _e = 0.04 m ² K/W]	
EN ISO 6946	7.7 W/(m ² K) [R _{si} = 0.13 m ² K/W] (horizontal heat flow)	10 W/(m ² K) [R _{si} = 0.1 m ² K/W] (Upward heat flow) 5.8 W/(m ² K) [R _{si} = 0.17 m ² K/W] (Downward heat flow)	25 W/(m ² K) [R _{se} = 0.04 m ² K/W] (Tables 5 and 7)	
EN 673	7.7 W/(m ² K) [1/h _i = 0.13 m ² K/W]	EN ISO 6946	25 W/(m ² K) [1/h _e = 0.04 m ² K/W]	
EN ISO 10077-1	7.7 W/(m ² K) [1/h _i = 0.13 m ² K/W]	10 W/(m ² K) [1/h _i = 0.1 m ² K/W]	25 W/(m ² K) [1/h _e = 0.04 m ² K/W]	
DTU 39	9 W/(m ² K)	11 W/(m ² K) (Upward flux) 6 W/(m ² K) (Downward flux)	11 W/(m ² K) (winter/mid-season) 13 W/(m ² K) (summer)	12 W/(m ² K) (winter/mid-season) 14 W/(m ² K) (summer)
ISO 15099		§8.5 $h = h_R + h_C$		§8.5 $h = h_R + h_C$
EN 52022-3		-		-
BELGIAN GUIDELINES		8 W/m ² K		16 W/m ² K
PILKINGTON INSTRUCTIONS		-		-

Solar radiation

The solar radiation per unit area is usually denoted as $G(t)$, whose typical values are recorded by standards in tables and graphs as a function of the season, time of day, facade orientation and inclination (see Table 4).

The French standard [55] furnishes detailed information about the global solar radiation and the diurnal temperature range only for France. The global solar radiation consists of direct and the diffuse radiation. The latter, caused by the clouds, ranges between 10% and 20% of the global solar radiation. The solar flux depends on the season, time of day, facade orientation and its inclination. In this case, a distinction is made if a transient regime or steady state are considered in the assessment, referring to tables or graphs in these two cases.

CNR DT 210 [121] suggests, in the absence of specific data for a specific location, using the maximum summer incident solar irradiance values on a vertical surface reported in tables for various latitudes and taken from UNI 10349 [153].

The Pilkington Instructions furnish the solar radiation intensity in graphs as a function of the location (United Kingdom or the rest of the world), the Belgian Guidelines [148] provide a value of 850 W/m² for inclined surfaces (from 10° to 75° with respect to the horizontal) and 750 W/m² for vertical surfaces, while ISO 15099 [12] and EN 52022-3 [144] provide reference values for winter and summer conditions (300 W/m² and 500 W/m², respectively). It should be noted that, although the solar radiation intensity is obviously variable through the day and depends on various parameters, as already anticipated, some of the cited standards instead furnish a maximum value for each season and/or for the facade orientation (Table 4).

Table 4. Solar radiation and consideration of shadows according to different standards.

	SOLAR RADIATION	SHADOWS
CNR DT 210	Max summer solar irradiance incident on a vertical surface referred to different latitudes (Table 4.13 taken from UNI 10349).	See Figure 9 of current paper
EN ISO 6946	-	-
EN 673	-	-
EN ISO 10077-1	-	-
DTU 39 ⁽¹⁾	<i>f</i> (season, daytime, facade orientation/inclination) SS: Table 6 (location/altitude) + corrective coeff. (Table 7) inclination/season (summer/winter) TR: Figure 23 (variable graphs)	10% of the global solar radiation in the shaded parts SS: min 75 W/m ² TR: Figure 24 <i>f</i> (season)
ISO 15099	Winter (§8.2.2) 300 W/m ² Summer (§8.2.3) 500 W/m ²	-
EN 52022-3	Reference BC (§6.4.6) 300 W/m ² Summer (§6.4.6) 500 W/m ²	-
BELGIAN GUIDELINES	10° < θ < 75° $G = 850$ W/m ² $\theta = 90^\circ G = 750$ W/m ² θ angle with respect to the horizontal	Coefficient <i>f</i> (shadow shape and glass type—single/double) Values: 1.1–1.5
PILKINGTON INSTRUCTIONS	Graphs <i>f</i> (location) in UK and rest of the world.	Shadow Factor No shadow: 1.0 Mobile shadow: 1.11 Static shadow: Figure 31

⁽¹⁾ SS: steady state; TR: transient regime.

Heat conduction

The heat conduction is usually neglected in simple analytical methods (particularly by the methods prescribed by the standards), thus inducing an overestimation of the thermal gradients.

Shadows

The only standard accounting for the presence of shadowed regions is the French one [55], but this neglects the conduction heat transfer among adjacent regions (Table 4). The same standard considers the temperature field as being constant in the thickness direction, only defining one temperature for each panel region, and it usually assumes that only a portion equal to the 10% of the global solar radiation strikes the shaded parts of the facade surface (i.e., diffuse flux for the shaded part, which, in the transient regime, is given by specific graphs as a function of the season). Other guidelines (for example, the Belgian one [148], which is no longer used, and the Pilkington Instructions [149]) account for the presence of shadows through the definition of corrective coefficients. Regarding the shadow shape, the Italian Guidelines [121] and the Belgian Guidelines [148] record an indicative classification of various types of shadows, from the least dangerous to the most dangerous (see Figure 9). According to [121], peak stress levels occur when the shadow covers less than 25% of the surface and includes over 25% of the perimeter. In general, the most critical situation is when a combination of horizontal, vertical or diagonal shadows exists, resulting in “V-shaped” shadows.

It should be noted that the approach followed by the standards for shadows is purely qualitative and a more refined approach is currently missing in Europe.

5.2.2. Determination of the Temperature Field

The available national and international standards and guidelines are partly outdated or contain simplified instructions and specifications for thermal stresses calculation in facade and roof glazing [116]. At present, considering the lack of alternative methods, the French standard [55], in combination with Vitrages Décision software and the John–Colvin method (English model), are used for the whole of Europe [116].

Codes and standards usually provide simple formulae to evaluate the glass temperature, while prescribing, via formulae and/or tables, values for the relevant coefficients and the (time-dependent) environmental parameters, such as temperature and solar radiation (see Section 5.2.1). Many models consider only the steady-state condition, neglecting the

presence of shadows and frame, and assume simplified (i.e., constant or linear) temperature profiles across the thickness.

The Pilkington Instructions [149] are one of the simplest assessment methods used to compute the thermal breakage behaviour of glass, but is only applicable to glasses manufactured by the Pilkington company. The calculation of temperature differences that lead to thermal breakage is determined from reference tables and graphs. The “Basic Temperature Difference” is found to be a function of the solar radiation intensity and the diurnal temperature range for the specific location from reference graphs. Then, the effects of blinds, drapes or medium/dark coloured back-ups, shadows and frame are considered using corrective coefficients. The resultant “Maximum Temperature Difference” is then compared to the “Safe Temperature Difference” reported in the Pilkington Instructions as a function of the glass type and its edge finishes.

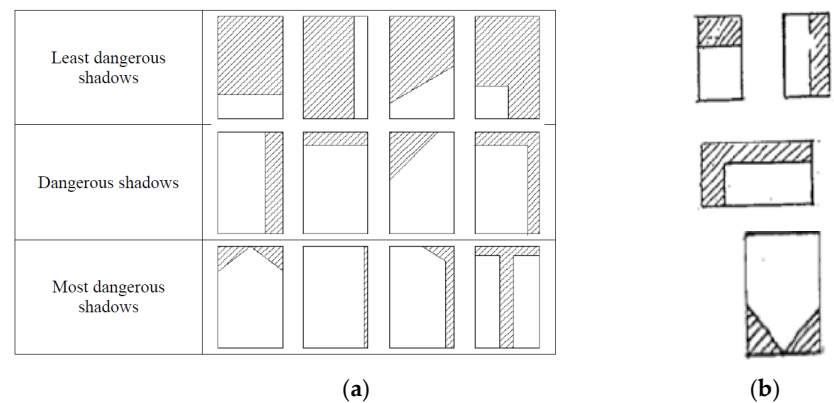


Figure 9. Examples of shadows on glass from: (a) CNR DT 210 [121] and (b) Belgian Guidelines [148].

The basis of calculation according to the Belgian Guidelines [148] relies on the difference in temperature between the visible part of the glass and the part in the window frame, which is based on the energy absorbed by the glazing and the variation in daytime temperatures. For single glazing:

$$\Delta T = \frac{G \cdot \alpha}{h_e + h_i} + \frac{A \cdot h_e}{h_e + h_i} \quad (18)$$

where:

- G Solar radiation maximum intensity (W/m^2) (for angles of 10° to 75° with respect to the horizontal, $G = 850 \text{ W}/\text{m}^2$, for 90° , $G = 750 \text{ W}/\text{m}^2$).
- α Absorption coefficient of the single glass (-), as defined in Section 2.1.3.
- A Maximum amplitude of the average diurnal temperature fluctuations over at least 10 years (K or $^\circ\text{C}$). This is a constant value depending on the geographical position (from 10 to 13 K).
- h_e Heat transfer coefficient at the outer surface ($h_e = 16 \text{ W}/\text{m}^2\text{K}$).
- h_i Heat transfer coefficient at the inner surface ($h_i = 8 \text{ W}/\text{m}^2\text{K}$).

The calculated temperature difference (ΔT) is then adjusted with corrective coefficients to account for the influence of blinds/curtains, frame and outside shadows.

One of the last available versions of the Project of European standard [150] provides a method for the determination of the basic temperature difference, which is dependent on “the solar energy absorption of glass, the solar radiation intensity, the heat transfer coefficients, the possible heating from radiant heaters, the diurnal temperature range”, as recorded in [52].

The most complete approaches to the evaluation of the temperature distribution in a multiple glazing are those proposed by the international standards [12,143,144] and by the French standard [55]. The former prescribes formulas based on the model proposed

by [48,154], relying on quite strict assumptions. The presence of the frame and projected shadows is neglected; therefore, the glass panel is considered as being entirely irradiated by the solar radiation. Furthermore, the glass temperature is considered as variable along the panel thickness, and the temperature profile is described in terms of its values at the back and front surface, whose relationship depends on the glass conductivity. Since it neglects heat storage, the method considers only the steady-state problem.

The French standard proposes three different levels of accuracy for the determination of the temperature field (*general*, *simple* and *simple manual methods*). The general method is the most comprehensive, as it considers the transient problem, and allows for calculation of the temperature in the central (hottest) panel areas, but it neglects the conduction heat transfer. The second approach (simple method) considers the steady-state problem, thus neglecting the heat storage, and is recommended for window frames with low thermal inertia (wood, PVC, aluminium, etc.). The third and simpler approach, referred to as the simple manual method, also neglects, in the case of multiple glazing, the radiant heat exchange between the various glass layers. Temperature calculation for different zones is performed manually.

The calculated temperature difference is then compared with the tabulated allowable temperature difference reported in §11.2 of the standard. Specifically, Tables 15–20 include data for various glass types (not heat-treated), considering shadowed and no shadowed areas, inclination and frames with low, medium and high thermal inertia. If the calculated temperature difference exceeds the allowable value in the table, then the chosen system is considered unsafe, as the probability of breakage is high.

5.2.3. Thermal Stress

Current standards are generally based on the use of very simple and approximate formula to determine the stress generated by the temperature difference in the glass pane [121,145], which should be evaluated according to Equations (14) and (15). The intensity of thermal stress in a glass pane is assumed to be proportional to the temperature difference ΔT between the hottest part (the central part, which receives solar radiation) and the coolest part (near the edges of the frame). Stress caused by ΔT is expressed in the following form:

$$\sigma_t = \Delta T E \alpha_T K_{\Delta T}, \quad (19)$$

where E is the elastic modulus of the glass ($\sim 70,000$ MPa), α_T is the thermal expansion coefficient ($\sim 9 \cdot 10^{-6} \text{ K}^{-1}$), and $K_{\Delta T}$ is a coefficient that accounts for the effects that can influence the value of the temperature gradient (shape of areas of shadow, frame characteristics, etc.); CNR DT 210 furnishes the values of this coefficient. Given the direct connection between temperature difference and induced stress, the admissible values for the resistance of glass to the effects of a temperature gradient can be directly expressed in terms of temperature gradient ΔT .

The French standard thermal stress assessment is based on an evaluation of stress based on the calculated temperature difference (for all methods, as per Section 5.2.2), which is then compared with the maximum allowable stress, whose evaluation is reported in §11.1 of the cited standard [55].

In Equation (19), $K_{\Delta T} = K_f K_o$, which depends on the presence of external shading (through K_o) and the heat capacity of the frames (through K_f). The following values are assumed:

Frame systems with low thermal inertia, no shades:	0.8.
Frame systems with low thermal inertia + shades:	0.9.
Frame systems with mean thermal inertia + shades:	1.0.
Frame systems with high thermal inertia + shades:	1.1.

The maximum allowable stress is given by:

$$\sigma_{adm} = K_v K_a \sigma_{vm} \quad (20)$$

with σ_{vm} as the allowable basic stress on glass, K_v as the sensibility coefficient of glass to thermal shock, and K_a accounting for inclination and support conditions. Such coefficients are reported in tables of the cited standard.

The American standard ASTM E2431 [155] proposes a very simple formula, based on [156], to directly evaluate the stress associated with the thermal loading. The stress is then equal to the maximum absorbed solar radiance αG , multiplied by a “thermal stress factor”, which is evaluated numerically and expressed in graphs as a function of the glass thickness, the edge bite and the edge-support conditions of the panel.

The calculated stress due to the thermal loadings must stay below the allowable stress corresponding to a certain probability of failure. This practice applies to monolithic and laminated glass of a rectangular shape and assumes that all glass edges are simply supported and free of damage. This very simple method neglects the heat conduction and convection, the irradiance from external and internal surfaces, and the effects of shadows [53].

5.3. Fire

5.3.1. Reaction to Fire

At present, all construction products are tested using the methods according to EN 13501-1 [157], which is relevant to the corresponding reaction to fire, allowing for classification according to the Commission Delegated Regulation (EU) 2016/364. There are seven classes (A1, A2, B, C, D, E and F), and EN 13501-1 provides the reaction to the fire methods used for all construction products, including products incorporated within building elements. EN 13501-1 foresees different test methods according to the specific reaction to fire class that must be obtained. It includes the non-combustibility test [158], the method used to determine the gross heat of combustion (Q_{PCS} , with PCS standing for “*Pouvoir Calorifique Supérieur*”) of products at constant volume in a bomb calorimeter [159], the SBI test for determining the reaction of construction products, excluding floorings, to fire when exposed to thermal attack by a single burning item [160], and the single-flame source test for determining the ignitability of products by direct small-flame impingement [161]. For the specific case of glass, two conditions can be distinguished:

1. Glass not containing organic materials, i.e., basic glass, coated glass, toughened glass, heat-strengthened glass, chemically strengthened glass, mirrors, glass blocks and paver units, are classified as A1 according to Commission Decision 96/603/EC, as amended by Commission Decision 2000/605/EC.
2. Glass containing a certain amount of organic material, i.e., laminated (safety) glass and insulating glass units, should be tested for their reaction to fire according to EN 13501-1.

According to CEN TC 129 and the glass industry, represented by Glass for Europe [162], EN 13823 (SBI test) is not appropriate to classify the reaction to fire of glass products and the full-scale room test (according to ISO 9705 [163] and EN 14390 [164]) is considered to better illustrate the behaviour of glass products.

5.3.2. Resistance to Fire

The second part of EN 13501 [165] focuses on the classification of construction elements based on fire-resistance testing. Classification is declared in minutes and is based on the load-bearing capacity (R), integrity (E) and thermal insulation (I). When required, optional performance parameters can be considered, such as the radiation (W), smoke leakage (S), mechanical action (M), self-closure (C), soot fire resistance (G) and fire protection ability (K).

In this case, EN 13501-2 recalls different test methods, including those included in EN 1363-1/3 [166–168], which establish the general principles for determining the fire resistance of various construction elements when subjected to standard fire exposure condition: EN 1364-1/5 [169–173] for non-loadbearing elements (walls, ceilings, curtain walling, etc.) and EN 1365-1/6 [174–179] for loadbearing elements (walls, floors and roofs, beams, columns, balconies and walkways and stairs).

The classification of facades (curtain walling) and external walls (including glazed elements) follows the indications of §7.5.3 of EN 13501-2 [165], and the performance criteria include integrity (E), thermal insulation (I) and radiation (W).

However, when talking about glass, and especially glass facades, the determination of an assessment method that goes beyond the current EN 13501-2 classification systems appears necessary.

In response to the lack of a harmonised testing standard or classification system, several EU countries have introduced their own tests to their national fire safety regulations. A total of 10 different test methods have been identified as being either currently in use or referenced in the regulations throughout Europe (see Table 5). This leads to the need for facade system manufacturers to carry out several fire tests to be able to sell their products in more than one country. There is currently a European project, formed in accordance with the Invitation to Tender for “Finalization of the European approach to assess the fire performance of facades” of the European commission (September 2019) [180], whose objective is to finalize the methodology used to assess the fire performance of facades including test methods and a classification proposal. As part of the project activities in [181], during a preliminary regulatory survey, the presence of any additional requirements to those in EN 13501-2 throughout Europe was searched, and it resulted that the main purposes of these requirements are:

- Limitation of fire spread on the surface and inside of the facade system;
- Demonstration of fire performance for systems that do not follow or cannot meet the fire performance characteristics for individual components, for example, insulation that cannot be categorized into the required reaction-to-fire class;
- Requirements regarding fire’s spread through facades from one room to another (through external surfaces, but also through cavities and facade floor junctions);
- Limitation or avoidance of falling parts and/or burning debris/droplets;
- Limitation of smouldering fires.

The requirements for falling parts and burning debris/droplets are particularly necessary to verify either (i) the protection provided by escape routes and for rescue services, and/or (ii) the prevention of secondary fires arising from burning debris/droplets.

The baseline test methods were initially defined as the BS 8414 and DIN 4102-20; however, an alternative assessment method was proposed to reduce the number of tests needed to satisfy the additional requirements for those Member States who do not use DIN 4102-20 or BS 8414. Such an alternative assessment method would combine as many of these options as possible in one test method, but modifications to the test rig and the test procedure will become necessary. The project is currently ongoing, and the result will lead to a harmonized assessment procedure and classification system for the fire performance of facades, which could be incorporated into the regulations of all Member States.

Table 5. Assessment methods applied by EU/EFTA Member States to assess the fire performance of facades.

Country	Assessment Method
Austria	ÖNORM B 3800-5 [182]
Czech Republic	ČSN ISO 13785-1 [183]
Denmark, Sweden, Norway	SP Fire 105 [184]
Finland	<ul style="list-style-type: none"> • SP Fire 105 • BS 8414 [185]
France	LEPIR 2 [186]
Germany	<ul style="list-style-type: none"> • DIN 4102-20 [187] • Technical regulation A 2.2.1.5 [188]
Hungary	MSZ 14800-6 [189]
Ireland	BS 8414 (BR 135)
Poland	PN-B-02867 [190]
Switzerland, Liechtenstein	<ul style="list-style-type: none"> • DIN 4102-20 • ÖNorm B 3800-5 • Prüfbestimmung für Aussenwandbekleidungssysteme (Test specifications for exterior wall-cladding systems)

6. Conclusions

In this paper, an extensive overview of aspects related to the evaluation of the response of structural and non-structural glass elements to thermal actions due to both climatic action and fire events has been proposed. In particular, the research has emphasized the multitude of factors that affect the determination of the thermal loads, which are related to the high number of heat exchange phenomena that come into play. These include convection and radiation exchanges with the surrounding environment, heat storage in the glazing element, and heat conduction at different temperatures. All these aspects should be taken into account to properly evaluate the complex time-dependent temperature field in the glazing, and, consequently, the state of thermal strain and stress in the glass panel. A state-of-the-art review is recorded that tries to summarize all the efforts made by various scientists in recent decades to address these important problems.

The last part of the paper emphasizes how the current regulatory scenario is characterized by conflicting rules, which do not allow for a uniformly accepted procedure to be defined that could assess the temperature field in the glazing and the consequent thermal stress. Furthermore, the standards provide a wide range of values for the basic coefficients adopted in these calculations. However, uniformly defined procedures for the calculation (stationary or transient, considering different time periods, etc.) are lacking, as well as assumptions regarding the simulation parameters. Moreover, there is no precise indication of how the thermal properties of frame, rebates, restraints, etc., should be taken into account in the evaluation of the temperature distribution and the consequent stress field in glass elements. Furthermore, the lack of harmonized recommendations for fire testing and fire endurance assessments using experiments still represents a major research gap. The above aspects are highlighted in Tables 1–4. Overall, these conditions lead also to major uncertainties regarding the possible generalized use of robust FE simulations to assess fire endurance [136].

Currently, a new European standard (Glass in building—Determination of the thermal shock resistance of glass panes—Calculation method) devoted to the assessment of methods of calculating temperature distribution and thermally induced stresses by temperature differentials in the glass pane, is under development.

Several open problems remain to be properly addressed and currently represent a major challenge for design of structural glass elements; these can represent objectives for future research developments. First of all, the reliability of a structural design depends on its ability to accurately determine the material failure strength; therefore, the evaluation of glass strength with respect to thermal actions is a major concern. Glass strength is dependent on the applied load; the effects of the loaded area (through the scale factor λ_{gA}), and of the length of the glass edge (through the scale factor λ_{gl}), the load duration and the environmental conditions (through the coefficient k_{mod}) should be taken into account and defined in the case of thermal actions.

Another important aspect is related to how the effect of climatic actions should be combined with other (permanent or variable) loads (with the corresponding factors for combination value of variable loads Ψ_0) in the case of structural glass elements. The general issue of load combinations in structural glass was pointed out in [191].

Last but not least, considering the high level of evidenced thermal model uncertainties, the approach to designs assisted by testing (as envisaged by Eurocode 0) could provide a valid support when aiming to obtain further knowledge of the discussed thermal problem. However, a proper experimental setup, obtained through precise loading specifications, testing arrangement and measurement methods, should be designed to consider all the aspects that influence the behaviour of glass (size effect, state of stress, static fatigue, load rate) [192]. Using such an experimental analysis to obtain a definition of the actual expectations in terms of structural strength is therefore a priority.

All the evidenced aspects of, and gaps in, the current scientific literature and standards, which have been dealt with in the paper, represent a possible field for future research, which

needs to be deepened to obtain reliable tools for the design and assessment of glazing in buildings subject to thermal loads.

Author Contributions: Conceptualization, writing – original draft preparation, writing – review and editing, visualization: L.G., A.F. and C.B. All authors have read and agreed to the published version of the manuscript.

Funding: This research received no external funding.

Data Availability Statement: There are no data to be shared.

Conflicts of Interest: The authors declare no conflict of interest.

References

1. Alwetaishi, M. Impact of glazing to wall ratio in various climatic regions: A case study. *J. King Saud Univ. Eng. Sci.* **2019**, *31*, 6–18. [[CrossRef](#)]
2. Hilliaho, K.; Nordquist, B.; Wallentèn, P.; Hamid, A.A.; Lahdensivu, J. Energy saving and indoor climate effects of an added glazed facade to a brick wall building: Case study. *J. Build. Eng.* **2016**, *7*, 246–262. [[CrossRef](#)]
3. Kim, D.; Cox, S.J.; Cho, H.; Yoon, J. Comparative investigation on building energy performance of double skin façade (DSF) with interior or exterior slat blinds. *J. Build. Eng.* **2018**, *20*, 411–423. [[CrossRef](#)]
4. Bedon, C.; Zhang, X.H.; Santos, F.; Honfi, D.; Kozłowski, M.; Arrigoni, M.; Figuli, L.; Lange, D. Performance of structural glass facades under extreme loads—Design methods, existing research, current issues and trends. *Constr. Build. Mater.* **2018**, *163*, 921–937. [[CrossRef](#)]
5. Stahn, D. Thermal stresses in heat-absorbing building glass subjected to solar radiation. In *Thermal Stresses in Severe Environments*; Springer: Berlin/Heidelberg, Germany, 1980; pp. 305–323.
6. Poláková, M.; Schäfer, S.; Elstner, M. Thermal Glass Stress Analysis—Design Considerations. In *Challenging Glass Conference Proceedings*; CGC: Sarasota, FL, USA, 2018; pp. 725–740.
7. Teotia, M.; Soni, R.K. Applications of finite element modelling in failure analysis of laminated glass composites: A review. *Eng Fail Anal* **2018**, *94*, 412–437. [[CrossRef](#)]
8. Schwind, G.; Paschke, F.; Schneider, J. Case Studies on the Thermally Induced Stresses in Insulating Glass Units via Numerical Calculation. In *Challenging Glass Conference, Proceedings of the Conference on Architectural and Structural Applications of Glass, Ghent, Belgium, 23–24 June 2022*; CGC: Sarasota, FL, USA, 2022; Volume 8.
9. Vengatesan, K. Windows Film to Glass: Numerical Simulation Software for Avoiding Thermal Stress. Master’s Thesis, IST Tecnico Lisboa, Lisbon, Portugal, 2017.
10. Bedon, C. Structural Glass Systems under Fire: Overview of Design Issues, Experimental Research, and Developments. *Adv. Civ. Eng.* **2017**, *2017*, 2120570. [[CrossRef](#)]
11. EU 305/2011; Regulation (EU) No 305/2011 of the European Parliament and of the Council of 9 March 2011 Laying down Harmonised Conditions for the Marketing of Construction Products and Repealing Council Directive 89/106/EEC. Official Journal of the European Union: Maastricht, The Netherlands, 2011.
12. ISO 15099; Thermal Performance of Windows, Doors and Shading Devices—Detailed Calculation. International Organization for Standardization: Geneva, Switzerland, 2003.
13. Li, M.Y.; Jiang, Y.J.; Coimbra, C.F.M. On the determination of atmospheric longwave irradiance under all-sky conditions. *Sol. Energy* **2017**, *144*, 40–48. [[CrossRef](#)]
14. Karn, A.; Chintala, V.; Kumar, S. An investigation into sky temperature estimation, its variation, and significance in heat transfer calculations of solar cookers. *Heat Transf.-Asian Res.* **2019**, *48*, 1830–1856. [[CrossRef](#)]
15. Berger, X.; Buriot, D.; Garnier, F. About the Equivalent Radiative Temperature for Clear Skies. *Sol. Energy* **1984**, *32*, 725–733. [[CrossRef](#)]
16. Gliha, O.; Kruczek, B.; Etemad, S.G.; Thibault, J. The effective sky temperature: An enigmatic concept. *Heat Mass Transf.* **2011**, *47*, 1171–1180. [[CrossRef](#)]
17. Swinbank, W.C. Long-wave radiation from clear skies. *Q. J. R. Meteorol. Soc.* **1963**, *89*, 339–348. [[CrossRef](#)]
18. Bergman, T.L.; Incropera, F.P.; DeWitt, D.P.; Lavine, A.S. *Fundamentals of Heat and Mass Transfer*; Wiley: New York, NY, USA, 2011.
19. Lienhard, J.H.I.; Lienhard, J.H.V. *A Heat Transfer Textbook*, 5th ed.; Phlogiston Press: London, UK, 2019.
20. EN ISO 6946; Building Components and Building Elements—Thermal Resistance and Thermal Transmittance—Calculation Methods. European Committee for Standardization (CEN): Brussels, Belgium, 2017.
21. Marino, C.; Nucara, A.; Pietrafesa, M.; Polimeni, E. The effect of the short wave radiation and its reflected components on the mean radiant temperature: Modelling and preliminary experimental results. *J. Build. Eng.* **2017**, *9*, 42–51. [[CrossRef](#)]
22. Churchill, S.W.; Chu, H.H.S. Correlating Equations for Laminar and Turbulent Free Convection from a Vertical Plate. *Int. J. Heat Mass. Transf.* **1975**, *18*, 1323–1329. [[CrossRef](#)]
23. Poirier, D.R.; Geiger, G.H. (Eds.) Correlations and Data for Heat Transfer Coefficients. In *Transport Phenomena in Materials Processing*; Springer International Publishing: Cham, Switzerland, 2016; pp. 247–279.

24. Loveday, D.L.; Taki, A.H. Convective heat transfer coefficients at a plane surface on a full-scale building facade. *Int. J. Heat Mass Transf.* **1996**, *39*, 1729–1742. [[CrossRef](#)]
25. Mirsadeghi, M.; Costola, D.; Blocken, B.; Hensen, J.L.M. Review of external convective heat transfer coefficient models in building energy simulation programs: Implementation and uncertainty. *Appl. Therm. Eng.* **2013**, *56*, 134–151. [[CrossRef](#)]
26. Defraeye, T.; Blocken, B.; Carmeliet, J. Convective heat transfer coefficients for exterior building surfaces: Existing correlations and CFD modelling. *Energy Convers. Manag.* **2011**, *52*, 512–522. [[CrossRef](#)]
27. Kahsay, M.T.; Bitsuamlak, G.; Tariku, F. Numerical analysis of convective heat transfer coefficient for building facades. *J. Build. Phys.* **2019**, *42*, 727–749. [[CrossRef](#)]
28. Montazeri, H.; Blocken, B.; Derome, D.; Carmeliet, J.; Hensen, J.L.M. CFD analysis of forced convective heat transfer coefficients at windward building facades: Influence of building geometry. *J. Wind Eng. Ind. Aerodyn.* **2015**, *146*, 102–116. [[CrossRef](#)]
29. Zhang, J.Y.; Zhao, L.; Deng, S.; Xu, W.C.; Zhang, Y. A critical review of the models used to estimate solar radiation. *Renew. Sustain. Energy Rev.* **2017**, *70*, 314–329. [[CrossRef](#)]
30. Compagnon, R. Solar and daylight availability in the urban fabric. *Energy Build.* **2004**, *36*, 321–328. [[CrossRef](#)]
31. Alqaed, S. Effect of annual solar radiation on simple facade, double-skin facade and double-skin facade filled with phase change materials for saving energy. *Sustain. Energy Technol.* **2022**, *51*, 101928. [[CrossRef](#)]
32. Unguresan, P.V.; Porumb, R.A.; Petreus, D.; Pocola, A.G.; Pop, O.G.; Balan, M.C. Orientation of Facades for Active Solar Energy Applications in Different Climatic Conditions. *J. Energy Eng.* **2017**, *143*. [[CrossRef](#)]
33. Valladares-Rendon, L.G.; Schmid, G.; Lo, S.L. Review on energy savings by solar control techniques and optimal building orientation for the strategic placement of facade shading systems. *Energy Build.* **2017**, *140*, 458–479. [[CrossRef](#)]
34. Perez, G.; Coma, J.; Sol, S.; Cabeza, L.F. Green facade for energy savings in buildings: The influence of leaf area index and facade orientation on the shadow effect. *Appl. Energy* **2017**, *187*, 424–437. [[CrossRef](#)]
35. Norris, D.J. Solar Radiation on Inclined Surfaces. *Sol. Energy* **1966**, *10*, 72–76. [[CrossRef](#)]
36. Demain, C.; Journée, M.; Bertrand, C. Evaluation of different models to estimate the global solar radiation on inclined surfaces. *Renew Energy* **2013**, *50*, 710–721. [[CrossRef](#)]
37. Maleki, S.A.M.; Hizam, H.; Gomes, C. Estimation of Hourly, Daily and Monthly Global Solar Radiation on Inclined Surfaces: Models Re-Visited. *Energies* **2017**, *10*, 134. [[CrossRef](#)]
38. Redweik, P.; Catita, C.; Brito, M. Solar energy potential on roofs and facades in an urban landscape. *Sol. Energy* **2013**, *97*, 332–341. [[CrossRef](#)]
39. Chow, T.T.; Chan, A.L.S.; Fong, K.F.; Lin, Z. Hong Kong solar radiation on building facades evaluated by numerical models. *Appl. Therm. Eng.* **2005**, *25*, 1908–1921. [[CrossRef](#)]
40. Han, J.M.; Choi, E.S.; Malkawi, A. CoolVox: Advanced 3D convolutional neural network models for predicting solar radiation on building facades. *Build. Simul.* **2022**, *15*, 755–768. [[CrossRef](#)]
41. Hofierka, J.; Sári, M.; Marecka, M. The solar radiation model for Open source GIS: Implementation and applications.
42. de Gracia, A.; Navarro, L.; Castell, A.; Ruiz-Pardo, A.; Alvarez, S.; Cabeza, L.F. Solar absorption in a ventilated facade with PCM. Experimental results. *Energy Proced* **2012**, *30*, 986–994. [[CrossRef](#)]
43. Speroni, A.; Mainini, A.G.; Zani, A.; Paolini, R.; Pagnacco, T.; Poli, T. Experimental Assessment of the Reflection of Solar Radiation from Facades of Tall Buildings to the Pedestrian Level. *Sustainability* **2022**, *14*, 5781. [[CrossRef](#)]
44. Hermanns, M.; del Ama, F.; Hernández, J.A. Analytical solution to the one-dimensional non-uniform absorption of solar radiation in uncoated and coated single glass panes. *Energy Build.* **2012**, *47*, 561–571. [[CrossRef](#)]
45. Alvarez, G.; Jimenez, D.N.; Estrada, C.A. Thermal performance of solar control coatings: A mathematical model and its experimental verification. *J. Phys. D Appl. Phys.* **1998**, *31*, 2249. [[CrossRef](#)]
46. Ismail, K.A.R.; Henriquez, J.R. Modeling and simulation of a simple glass window. *Sol. Energy Mater. Sol. Cells* **2003**, *80*, 355–374. [[CrossRef](#)]
47. Powles, R.; Curcija, D.; Kohler, C. *Solar Absorption in Thick and Multilayered Glazings*; LBNL: Berkeley, CA, USA, 2002.
48. Wright, J.L. *Calculating Center-Glass Performance Indices of Windows*; Ashrae Transactions 104; UWSpace: Washington, DC, USA, 1998; pp. 1230–1241.
49. Fanchiotti, A.; Messina, G.; Volpe Rinonapoli, C. A computer code for determining the effect of shadows on the availability of solar radiation on facades of buildings. In *Passive and Low Energy Architecture*; Yannas, S., Ed.; Elsevier: Pergamon, Turkey, 1983; pp. 603–610. [[CrossRef](#)]
50. Trujillo, J.H.S. Solar performance and shadow behaviour in buildings. Case study with computer modelling of a building in Loranca, Spain. *Build Environ* **1998**, *33*, 117–130. [[CrossRef](#)]
51. Heisler, G.M. Effects of Individual Trees on the Solar-Radiation Climate of Small Buildings. *Urban Ecol.* **1986**, *9*, 337–359. [[CrossRef](#)]
52. Anastasiou, C. Thermal Breakage of Glass. Master's Thesis, Delft University of Technology, Delft, The Netherlands, 2016.
53. Vandebroek, M.; Belis, J.; Louter, C. Thermal breakage of glass. In *COST Action TU0905 Mid-Term Conference on Structural Glass*; Routledge: London, UK, 2013; pp. 563–569.
54. Galuppi, L.; Maffei, M.; Royer-Carfagni, G. Enhanced engineered calculation of the temperature distribution in architectural glazing exposed to solar radiation. *Glass Struct. Eng.* **2021**, *6*, 425–448. [[CrossRef](#)]
55. NF DTU 39 P3; Building Works—Glazing and Mirror-Glass Works—Part 3: Calculation Memorandum for Thermal Stress [Travaux de Vitrierie-Miroiterie—Partie 3: Mémento Calculs des Contraintes Thermiques]. Association française de normalisation (AFNOR), 2006.

56. Galuppi, L.; Maffei, M.; Royer-Carfagni, G. Engineered calculation of the uneven in-plane temperatures in Insulating Glass Units for structural design. *Glass Struct. Eng.* **2022**, *7*, 71–99. [[CrossRef](#)]
57. Manz, H. On minimizing heat transport in architectural glazing. *Renew. Energy* **2008**, *33*, 119–128. [[CrossRef](#)]
58. Galuppi, L.; Royer-Carfagni, G. Thermal analysis of architectural glazing in uneven conditions based on Biot’s variational principle: Part I—Description of the finite element modelling. *Glass Struct. Eng.* **2023**, *8*, 41–56. [[CrossRef](#)]
59. Galuppi, L.; Royer-Carfagni, G. Thermal analysis of architectural glazing in uneven conditions based on Biot’s variational principle: Part II—Validation and case-studies. *Glass Struct. Eng.* **2023**, *8*, 57–80. [[CrossRef](#)]
60. Foraboschi, P. Analytical modeling to predict thermal shock failure and maximum temperature gradients of a glass panel. *Mater. Des.* **2017**, *134*, 301–319. [[CrossRef](#)]
61. Kozłowski, M.; Bedon, C. Sensitivity to Input Parameters of Failure Detection Methods for Out-of-Plane Loaded Glass Panels in Fire. *Fire* **2021**, *4*, 5. [[CrossRef](#)]
62. EN 572-1; Glass in Building—Basic Soda-Lime Silicate Glass Products—Part 1: Definitions and General Physical and Mechanical Properties (EN 572-1:2012+A1:2016). European Committee for Standardization (CEN): Brussels, Belgium, 2012.
63. Krauter, S.; Araujo, R.G.; Schroer, S.; Hanitsch, R.; Salhi, M.J.; Triebel, C.; Lemoine, R. Combined photovoltaic and solar thermal systems for facade integration and building insulation. *Sol. Energy* **1999**, *67*, 239–248. [[CrossRef](#)]
64. Infield, D.; Mei, L.; Eicker, U. Thermal performance estimation for ventilated PV facades. *Sol. Energy* **2004**, *76*, 93–98. [[CrossRef](#)]
65. Gasworth, S.; Tankala, T. Reduced Steady State Heating and Air Conditioning Loads via Reduced Glazing Thermal Conductivity. *SAE Tech. Pap.* **2011**. [[CrossRef](#)]
66. Bedon, C.; Louter, C. Thermo-mechanical Numerical Modelling of Structural Glass under Fire—Preliminary Considerations and Comparisons. In Proceedings of the Challenging Glass Conference 6: International Conference on Architectural and Structural Applications of Glass; TU Delft: Delft, The Netherlands, 2018; pp. 513–524.
67. Louter, C.; Bedon, C.; Kozłowski, M.; Nussbaumer, A. Structural response of fire-exposed laminated glass beams under sustained loads; exploratory experiments and FE-Simulations. *Fire Saf. J.* **2021**, *123*, 103353. [[CrossRef](#)]
68. Sjöström, J.; Kozłowski, M.; Honfi, D.; Lange, D.; Albrektsson, J.; Lenk, P.; Eriksson, J. Fire Resistance Testing of a Timber-Glass Composite Beam. *Int. J. Struct. Glass Adv. Mater. Res.* **2020**, *4*, 24–40. [[CrossRef](#)]
69. ISO 834-1/14; Fire-Resistance Tests—Elements of Building Construction. International Organization for Standardization: Geneva, Switzerland, 2020.
70. Kozłowski, M.; Bedon, C.; Honfi, D. Numerical Analysis and 1D/2D Sensitivity Study for Monolithic and Laminated Structural Glass Elements under Thermal Exposure. *Materials* **2018**, *11*, 1447. [[CrossRef](#)]
71. Honfi, D.; Sjöström, J.; Bedon, C.; Kozłowski, M. Experimental and Numerical Analysis of Thermo-Mechanical Behaviour of Glass Panes Exposed to Radiant Heating. *Fire* **2022**, *5*, 124. [[CrossRef](#)]
72. Vedrtnam, A.; Bedon, C.; Youssef, M.A.; Wamiq, M.; Sabsabi, A.; Chaturvedi, S. Experimental and numerical structural assessment of transparent and tinted glass during fire exposure. *Constr. Build. Mater.* **2020**, *250*, 118918. [[CrossRef](#)]
73. Vedrtnam, A.; Bedon, C.; Youssef, M.A.; Chaturvedi, S. Effect of non-uniform temperature exposure on the out-of-plane bending performance of ordinary laminated glass panels. *Comput. Struct.* **2021**, *275*. [[CrossRef](#)]
74. Manz, H.; Brunner, S.; Wullschlegel, L. Triple vacuum glazing: Heat transfer and basic mechanical design constraints. *Sol. Energy* **2006**, *80*, 1632–1642. [[CrossRef](#)]
75. Blanus, P.; Goss, W.P.; Roth, H.; Weitzmann, P.; Jensen, C.F.; Svendsen, S.; Elmahdy, H. Comparison between ASHRAE and ISO thermal transmittance calculation methods. *Energy Build.* **2007**, *39*, 374–384. [[CrossRef](#)]
76. Gasparella, A.; Pernigotto, G.; Cappelletti, F.; Romagnoni, P.; Baggio, P. Analysis and modelling of window and glazing systems energy performance for a well insulated residential building. *Energy Build.* **2011**, *43*, 1030–1037. [[CrossRef](#)]
77. Garay, R.; Uriarte, A.; Apraiz, I. Performance assessment of thermal bridge elements into a full scale experimental study of a building facade. *Energy Build.* **2014**, *85*, 579–591. [[CrossRef](#)]
78. Brandl, D.; Mach, T.; Grobbauer, M.; Hochenauer, C. Analysis of ventilation effects and the thermal behaviour of multifunctional facade elements with 3D CFD models. *Energy Build.* **2014**, *85*, 305–320. [[CrossRef](#)]
79. Galuppi, L.; Royer-Carfagni, G. Biot’s Variational Method to determine the thermal strain in layered glazings. *Int. J. Solids Struct.* **2022**, *249*, 111657. [[CrossRef](#)]
80. Gatewood, B.E. *Thermal Stresses*; McGraw-Hill Public: New York, NY, USA, 1957.
81. Ebisawa, J.; Ando, E. Solar control coating on glass. *Curr. Opin. Solid State* **1998**, *3*, 386–390. [[CrossRef](#)]
82. Zheng, L.; Xiong, T.; Shah, K.W. Transparent nanomaterial-based solar cool coatings: Synthesis, morphologies and applications. *Sol. Energy* **2019**, *193*, 837–858. [[CrossRef](#)]
83. Tong, S.W.; Goh, W.P.; Huang, X.H.; Jiang, C.Y. A review of transparent-reflective switchable glass technologies for building facades. *Renew. Sustain. Energy Rev.* **2021**, *152*, 111615. [[CrossRef](#)]
84. Alvarez, G.; Flores, J.J.; Estrada, C.A. The thermal response of laminated glass with solar control coating. *J. Phys. D Appl. Phys.* **1998**, *31*, 3057–3065. [[CrossRef](#)]
85. Galuppi, L.; Royer-Carfagni, G. Betti’s Analytical Method for the load sharing in double glazed units. *Comput. Struct.* **2020**, *235*. [[CrossRef](#)]
86. Galuppi, L. Practical expressions for the design of DGUs. The BAM approach. *Eng. Struct.* **2020**, *221*, 110993. [[CrossRef](#)]

87. Morse, S.M.; Norville, H.S. Comparison of methods to determine load sharing of insulating glass units for environmental loads. *Glass Struct. Eng.* **2016**, *1*, 315–329. [[CrossRef](#)]
88. McMahon, S.; Norville, H.S.; Morse, S.M. Experimental Investigation of Load Sharing in Insulating Glass Units. *J. Archit. Eng.* **2018**, *24*. [[CrossRef](#)]
89. Galuppi, L.; Royer-Carfagni, G. Green's functions for the load sharing in multiple insulating glazing units. *Int. J. Solids Struct.* **2020**, *206*, 412–425. [[CrossRef](#)]
90. Wright, J.L. *A Correlation to Quantify Convective Heat Transfer between Vertical Window Glazings*; Ashrae Transactions 1996; UWSpace: Washington, DC, USA, 1996; Volume 102, pp. 940–946.
91. Rosenfeld, J.L.J.; Platzer, W.J.; Van Dijk, H.; Maccari, A. Modelling the optical and thermal properties of complex glazing: Overview of recent developments. *Sol. Energy* **2000**, *69*, 1–13. [[CrossRef](#)]
92. Xaman, J.; Alvarez, G.; Lira, L.; Estrada, C. Numerical study of heat transfer by laminar and turbulent natural convection in tall cavities of facade elements. *Energy Build.* **2005**, *37*, 787–794. [[CrossRef](#)]
93. Respondek, Z. Heat Transfer Through Insulating Glass Units Subjected to Climatic Loads. *Materials* **2020**, *13*, 286. [[CrossRef](#)]
94. Manz, H. Numerical simulation of heat transfer by natural convection in cavities of facade elements. *Energy Build.* **2003**, *35*, 305–311. [[CrossRef](#)]
95. Gan, G.H. Thermal transmittance of multiple glazing: Computational fluid dynamics prediction. *Appl. Therm. Eng.* **2001**, *21*, 1583–1592. [[CrossRef](#)]
96. Maruyama, S.; Mori, Y.; Chikira, C.; Sakai, S. Combined nongray radiative and conductive heat transfer in multiple glazing taking into account specular reflection and absorption. *Heat Transf.-Asian Res.* **2003**, *32*, 712–726. [[CrossRef](#)]
97. Siegel, R. Net Radiation Method for Transmission through Partially Transparent Plates. *Sol. Energy* **1973**, *15*, 273–276. [[CrossRef](#)]
98. Wijesundera, N.E. A net radiation method for the transmittance and absorptivity of a series of parallel regions. *Sol. Energy* **1975**, *17*, 75–77. [[CrossRef](#)]
99. Edwards, D.K. Solar Absorption by Each Element in an Absorber-Coverglass Array. *Sol. Energy* **1977**, *19*, 401–402. [[CrossRef](#)]
100. Wright, J.L.; Kotey, N.A. *Solar Absorption by Each Element in a Glazing/Shading Layer Array*; Ashrae Transactions 2006; UWSpace: Washington, DC, USA, 2006; Volume 112.
101. Saelens, D.; Carmeliet, J.; Hens, H. Energy performance assessment of multiple-skin facades. *Hvac&R Res.* **2003**, *9*, 167–185. [[CrossRef](#)]
102. Saelens, D.; Roels, S.; Hens, H. The inlet temperature as a boundary condition for multiple-skin facade modelling. *Energy Build.* **2004**, *36*, 825–835. [[CrossRef](#)]
103. Manz, H.; Frank, T. Thermal simulation of buildings with double-skin facades. *Energy Build.* **2005**, *37*, 1114–1121. [[CrossRef](#)]
104. Saelens, D.; Roels, S.; Hens, H. Strategies to improve the energy performance of multiple-skin facades. *Build Environ* **2008**, *43*, 638–650. [[CrossRef](#)]
105. Feldmeier, F. Insulating units exposed to wind and weather-load sharing and internal loads. In *Glass Processing Days*; Elsevier: Amsterdam, The Netherlands, 2003.
106. Feldmeier, F. Klimabelastung und Lastverteilung bei Mehrscheiben-Isolierglas. *Stahlbau* **2006**, *75*, 467–478. [[CrossRef](#)]
107. Zacchei, E.; Galuppi, L. Influence of climatic actions on the dynamic response of Insulating Glass Units. Submitted. 2022.
108. Keski-Rahkonen, O. Breaking of window glass close to fire. *Fire Mater.* **1988**, *12*, 61–69. [[CrossRef](#)]
109. Drysdale, D. *An Introduction to Fire Dynamics*; Wiley: New York, NY, USA, 2011.
110. Strobel, C.S.; Abadie, M.O.; Mendes, N. Absorption of solar radiation in thick and multilayered glazing. *Build. Simul.* **2007**, *1–3*, 238–244.
111. Debuyser, M.; Sjostrom, J.; Lange, D.; Honfi, D.; Sonck, D.; Belis, J. Behaviour of monolithic and laminated glass exposed to radiant heating. *Constr. Build. Mater.* **2017**, *130*, 212–229. [[CrossRef](#)]
112. Nammi, S.K.; Shirvani, H.; Shirvani, A.; Edwards, G.; Whitty, J.P.M. *Verification of Calculation Code THERM in Accordance with BS EN ISO 10077-2*; Anglia Ruskin University: Chelmsford, UK, 2014.
113. Jeffers, A.E. Heat transfer element for modeling the thermal response of non-uniformly heated plates. *Finite Elem. Anal. Des.* **2013**, *63*, 62–68. [[CrossRef](#)]
114. Jeffers, A.E. Triangular Shell Heat Transfer Element for the Thermal Analysis of Nonuniformly Heated Structures. *J. Struct. Eng.* **2016**, *142*, 04015084. [[CrossRef](#)]
115. Liu, N.; Beata, P.A.; Jeffers, A.E. A mixed isogeometric analysis and control volume approach for heat transfer analysis of nonuniformly heated plates. *Numer. Heat Transf. Part B Fundam.* **2019**, *75*, 347–362. [[CrossRef](#)]
116. Ensslen, F.; Schwind, G.; Schneider, J.; Beinert, A.; Mahfoudi, A.; Lorenz, E.; Herzberg, W.; Elstner, M.; Polakova, M.; Schäfer, S.; et al. Joint Research Project (in progress): Draft Standard for Determining the Thermal Stress of Glass and Glass-Glass PV Modules (BIPV) in the Construction Industry. In *Challenging Glass Conference 8, Proceedings of the Conference on Architectural and Structural Applications of Glass, Ghent, Belgium, 23–24 June 2022*; Ghent University: Ghent, Belgium, 2022.
117. Pisano, G.; Royer Carfagni, G. The statistical interpretation of the strength of float glass for structural applications. *Constr. Build. Mater.* **2015**, *98*, 741–756. [[CrossRef](#)]
118. Pisano, G.; Bonati, A.; Royer-Carfagni, G. The effect of size and stress state on the strength of architectural glass. Experiments versus theory. *Constr. Build. Mater.* **2021**, *283*, 122635. [[CrossRef](#)]
119. Vandebroek, M.; Belis, J.; Louter, C.; Van Tendeloo, G. Experimental validation of edge strength model for glass with polished and cut edge finishing. *Eng. Fract. Mech.* **2012**, *96*, 480–489. [[CrossRef](#)]

120. Vandebroek, M.; Louter, C.; Caspeele, R.; Ensslen, F.; Belis, J. Size effect model for the edge strength of glass with cut and ground edge finishing. *Eng. Struct.* **2014**, *79*, 96–105. [[CrossRef](#)]
121. *CNR-DT 210*; Guide for the Design, Construction and Control of Buildings with Structural Glass Elements. Italian National Research Council (CNR): Rome, Italy, 2013.
122. Carlson, D.E. Linear Thermoelasticity. In *Linear Theories of Elasticity and Thermoelasticity: Linear and Nonlinear Theories of Rods, Plates, and Shells*; Truesdell, C., Ed.; Springer: Berlin/Heidelberg, Germany, 1973; pp. 297–345. [[CrossRef](#)]
123. Carter, J.P.; Booker, J.R. Finite element analysis of coupled thermoelasticity. *Comput. Struct.* **1989**, *31*, 73–80. [[CrossRef](#)]
124. Galuppi, L.; Royer-Carfagni, G. Thermal and elastic modelling of architectural glass unevenly heated by the environment. Formal symmetry from Biot's variational principle. *Int. J. Solids Struct.* **2022**; *under review*. Available online: <https://ssrn.com/abstract=4261726> (accessed on 12 March 2023).
125. Pelayo, F.; Lamela-Rey, M.J.; Muniz-Calvente, M.; Lopez-Aenlle, M.; Alvarez-Vazquez, A.; Fernandez-Canteli, A. Study of the time-temperature-dependent behaviour of PVB: Application to laminated glass elements. *Thin Wall Struct.* **2017**, *119*, 324–331. [[CrossRef](#)]
126. Serafinavicius, T.; Lebet, J.P.; Louter, C.; Lenkimas, T.; Kuranovas, A. Long-term laminated glass four point bending test with PVB, EVA and SG interlayers at different temperatures. *Procedia Eng.* **2013**, *57*, 996–1004. [[CrossRef](#)]
127. Asik, M.Z.; Tezcan, S. Laminated glass beams: Strength factor and temperature effect. *Comput. Struct.* **2006**, *84*, 364–373. [[CrossRef](#)]
128. Guo, S.L.; Wang, B.L.; Wang, K.F.; Li, J.E. Coupling effects of dual-phase-lag heat conduction and property difference on thermal shock fracture of coating/substrate structures. *Int. J. Solids Struct.* **2018**, *152*, 238–247. [[CrossRef](#)]
129. Frey, C.; Dolling, S.; Lestakova, M.; Becker, W. Free-edge crack onset induced by thermal loading. *Int. J. Solids Struct.* **2021**, *230*. [[CrossRef](#)]
130. Ivanov, I.V. Analysis, modelling, and optimization of laminated glasses as plane beam. *Int. J. Solids Struct.* **2006**, *43*, 6887–6907. [[CrossRef](#)]
131. Galuppi, L.; Royer-Carfagni, G.F. Effective thickness of laminated glass beams: New expression via a variational approach. *Eng. Struct.* **2012**, *38*, 53–67. [[CrossRef](#)]
132. Ivanov, I.V.; Velchev, D.S.; Georgiev, N.G.; Ivanov, I.D.; Sadowski, T. A plate finite element for modelling of triplex laminated glass and comparison with other computational models. *Meccanica* **2016**, *51*, 341–358. [[CrossRef](#)]
133. Wang, Q.; Zhang, Y.; Wang, Y.; Sun, J.; He, L. Dynamic three-dimensional stress prediction of window glass under thermal loading. *Int. J. Therm. Sci.* **2012**, *59*, 152–160. [[CrossRef](#)]
134. Bedon, C.; Louter, C. Fire endurance analysis of ordinary structural glass elements. In Proceedings of the Applications of Structural Fire Engineering—Proceeding of the International Conference in Ljubljana, Ljubljana, Slovenia, 10–11 June 2021; pp. 155–160.
135. Wang, Q.S.; Chen, H.D.; Wang, Y.; Sun, J.H. Thermal shock effect on the glass thermal stress response and crack propagation. *Procedia Eng.* **2013**, *62*, 717–724. [[CrossRef](#)]
136. Bedon, C.; Louter, C. Thermo-mechanical numerical analyses in support of fire endurance assessment of ordinary soda-lime structural glass elements. *J. Struct. Fire Eng.* **2023**; *in print*.
137. EN 572-9 Glass in Building—Basic Soda Lime Silicate Glass Products—Part 9: Evaluation of Conformity/Product Standard; European Committee for Standardization (CEN): Brussels, Belgium, 2004.
138. EN 673; Glass in building—Determination of Thermal Transmittance (U Value)—Calculation Method. European Committee for Standardization (CEN): Brussels, Belgium, 2011.
139. EN ISO 10077-2; Thermal Performance of Windows, Doors and Shutters—Calculation of Thermal Transmittance—Part 2: Numerical Method for Frames. European Committee for Standardization (CEN): Brussels, Belgium, 2017.
140. EN 410; Glass in building—Determination of Luminous and Solar Characteristics of Glazing. European Committee for Standardization (CEN): Brussels, Belgium, 2011.
141. ISO 9050; Glass in Building—Determination of Light Transmittance, Solar Direct Transmittance, Total Solar Energy Transmittance, Ultraviolet Transmittance and Related Glazing Factors. International Organization for Standardization: Geneva, Switzerland, 2003.
142. EN 12898; Glass in Building—Determination of the Emissivity. European Committee for Standardization (CEN): Brussels, Belgium, 2019.
143. EN ISO 52022-1; Energy Performance of Buildings—Thermal, Solar and Daylight Properties of Building Components and Elements—Part 1: Simplified Calculation Method of the Solar and Daylight Characteristics for Solar Protection Devices Combined with Glazing. European Committee for Standardization (CEN): Brussels, Belgium, 2017.
144. EN ISO 52022-3; Energy Performance of Buildings—Thermal, Solar and Daylight Properties of Building Components and Elements—Part 3: Detailed Calculation Method of the Solar and Daylight Characteristics for Solar Protection Devices Combined with Glazing. European Committee for Standardization (CEN): Brussels, Belgium, 2017.
145. CEN/TS 19100-1; Design of Glass Structures—Part 1: Basis of Design and Materials. European Committee for Standardization (CEN): Brussels, Belgium, 2021.
146. CEN/TS 19100-2; Design of Glass Structures—Part 2: Design of Out-of-Plane Loaded Glass Components. European Committee for Standardization (CEN): Brussels, Belgium, 2021.
147. CEN/TS 19100-3; Design of Glass Structures—Part 3: Design of in-Plane Loaded Glass Components and Their Mechanical joints. European Committee for Standardization (CEN): Brussels, Belgium, 2021.
148. FIV 01; Belgian Guidelines. Fédération de l'Industrie du Verre (FIV): Bruxelles, Belgium, 1997.
149. CEN/TC129/WG8-N180E; Glass and Thermal Safety—Pilkington Instructions. Pilkington: Houston, TX, U, 2004.
150. prEN. Glass in Building—Thermal stress calculation method NA 005-09-25 AA N 854, CEN/TC129/WG8—N1326: 2004.

151. UNI 5364; Impianti di Riscaldamento ad Acqua Calda. Regole per la Presentazione Dell' Offerta e per il Collaudo. Ente Italiano di Normazione: Milano Italy, 1976.
152. EN ISO 10077-1; Thermal Performance of Windows, Doors and Shutters—Calculation of Thermal Transmittance—Part 1: General. European Committee for Standardization (CEN): Brussels, Belgium, 2017.
153. UNI 10349-1; Riscaldamento e Raffrescamento Degli Edifici—Dati Climatici—Parte 1: Medie Mensili per la Valutazione Della Prestazione Termo-Energetica Dell'edificio e Metodi per Ripartire L'irradianza Solare Nella Frazione Diretta e Diffusa e per Calcolare L'irradianza Solare su di una Superficie Inclinata. Ente Italiano di Normazione: Milano. Italy, 2016.
154. Hollands, K.T.; Wright, J.; Granqvist, C. Glazings and coatings. In *Solar Energy: The State of the Art*; James & James Scientific Publishers: London, UK, 2001.
155. ASTM E2431; Standard Practice for Determining the Resistance of Single Glazed Annealed Architectural Flat Glass to Thermal Loadings. ASTM International: West Conshohocken, PA, USA, 2012.
156. Lingnell, A.W.; Beason, W.L. A Method of Evaluation for Thermal Stress in Monolithic Annealed Glass. Proceedings of Glass Processing Days, Tampere, Finland, 15–18 June 2003; pp. 291–293.
157. EN 13501-1; Fire Classification of Construction Products and Building Elements—Part 1: Classification Using Data from Reaction to fire Tests. European Committee for Standardization (CEN): Brussels, Belgium, 2018.
158. EN ISO 1182; Reaction to Fire Tests for Products–Non-Combustibility Tes. European Committee for Standardization (CEN): Brussels, Belgium, 2020.
159. EN ISO 1716; Reaction to Fire Tests for Products–Determination of the Gross Heat of Combustion (Calorific Value). European Committee for Standardization (CEN): Brussels, Belgium, 2018.
160. EN 13823; Reaction to fire Tests for Building Products–Building Products Excluding Floorings Exposed to the Thermal Attack by a Single Burning Item. CEN, 2020.
161. EN ISO 11925-2; Reaction to Fire Tests–Ignitability of Products Subjected to Direct Impingement of Flame—Part 2: Single-Flame Source Test. European Committee for Standardization (CEN): Brussels, Belgium, 2020.
162. Glass for Europe. *Classification of reaction to fire of glass products_Recommendation from Glass for Europe*; Position Paper; Glass for Europe: Etterbeek, Belgium, 2015.
163. ISO 9705; Fire Tests—Full-Scale Room Test for Surface Products [Withdrawn]. International Organization for Standardization: Geneva, Switzerland, 1993.
164. EN 14390; Fire Test—LARGE-Scale Room Reference Test for Surface Products. European Committee for Standardization (CEN): Brussels, Belgium, 2007.
165. EN 13501-2; Fire Classification of Building Products from Fire Resistance Tests without Ventilation. European Committee for Standardization (CEN): Brussels, Belgium, 2016.
166. EN 1363-1; Fire Resistance Tests—Part 1: General Requirements. European Committee for Standardization (CE: Brussels, Belgium, 2020.
167. EN 1363-2; Fire Resistance Tests—Part 2: Alternative and Additional Procedures. European Committee for Standardization (CEN): Brussels, Belgium, 1999.
168. EN 1363-3; Fire Resistance Tests—Part 3: Verification of Furnace Performance. European Committee for Standardization (CEN): Brussels, Belgium, 1998.
169. EN 1364-1; Fire Resistance Tests for Non-Loadbearing Elements—Part 1: Walls. European Committee for Standardization (CEN): Brussels, Belgium, 2015.
170. EN 1364-2; Fire Resistance Tests for Non-Loadbearing Elements—Part 2: Ceilings. European Committee for Standardization (CEN): Brussels, Belgium, 2018.
171. EN 1364-3; Fire Resistance Tests for Non-Loadbearing Elements—Part 3: Curtain Walling—Full Configuration (Complete Assembly). European Committee for Standardization (CEN): Brussels, Belgium, 2014.
172. EN 1364-4; Fire Resistance Tests for Non-Loadbearing Elements—Part 4: Curtain Walling—Part Configuration. European Committee for Standardization (CEN): Brussels, Belgium, 2014.
173. EN 1364-5; Fire Resistance Tests for Non-Loadbearing Elements—Part 5: Air Transfer Grille. European Committee for Standardization (CEN): Brussels, Belgium, 2017.
174. EN 1365-1:2012/AC:2013; Fire Resistance Tests for Loadbearing Elements—Part 1: Walls. European Committee for Standardization (CEN): Brussels, Belgium, 2014.
175. EN 1365-2; Fire Resistance Tests for Loadbearing Elements—Part 2: Floors and Roofs. European Committee for Standardization (CEN): Brussels, Belgium, 2014.
176. EN 1365-3; Fire Resistance Tests for Loadbearing Elements—Part 3: Beams. European Committee for Standardization (CEN): Brussels, Belgium, 1999.
177. EN 1365-4; Fire Resistance Tests for Loadbearing Elements—Part 4: Columns. European Committee for Standardization (CEN): Brussels, Belgium, 1999.
178. EN 1365-5; Fire Resistance Tests for Loadbearing Elements, Part 5—Balconies and Walkways. European Committee for Standardization (CEN): Brussels, Belgium, 2004.
179. EN 1365-6; Fire Resistance Tests for Loadbearing Elements, Part 6—Stairs. European Committee for Standardization (CEN): Brussels, Belgium, 2004.

180. European Commission. “Finalisation of the European Approach to Assess the Fire Performance of Facades” Call for Tenders No 761/PP/GRO/IMA/19/1133/11140; European Commission: Brussels, Belgium, 2019.
181. Anderson, J.; Boström, L.; Chiva, R.; Guillaume, E.; Colwell, S.; Hofmann, A.; Tóth, P. European approach to assess the fire performance of façades. *Fire Mater.* **2021**, *45*, 598–608. [[CrossRef](#)]
182. ÖNORM B 3800-5; Fire Behaviour of Building Materials and Components—Part 5: Fire Behaviour of Facades—Requirements, Tests and Evaluations. Austrian Standard: Vienna, Austria, 2013.
183. ČSN ISO 13785-1; Reaction-to-Fire Tests for Façades—Part 1: Intermediate-Scale Test. Czech Standard Institute: Brno, Czech Republic, 2010.
184. SP FIRE 105; Method for fire Testing of Façade Materials. Department of Fire Technology, Swedish National Testing and Research Institute: Borås, Sweden, 1985.
185. BS 8414; Fire Performance of External Cladding Systems. British Standard Organisation: London, UK, 2015.
186. LEPiR 2; Essais de Résistance au feu de Façade.
187. DIN 4102-20; Fire Behaviour of Building Materials and Building Components—Part 20: Complementary Verification for the Assessment of the Fire Behaviour of External Wall Claddings [Brandverhalten von Baustoffen und Bauteilen—Teil 20: Ergänzender Nachweis für die Beurteilung des Brandverhaltens von Außenwandbekleidungen]. Deutsches Institut für Normung: Berlin, Germany, 2017.
188. Technical Regulation A 2.2.1.5; Musterverwaltungsvorschrift mit Technischen Baubestimmungen, Anhang 5 WDVS mit EPS, Sockelbrandprüfverfahren.
189. MSZ 14800-6; Fire Resistance Tests. Part 6: Fire Propagation Test for Building Façades Magyar Szabványügyi Testület (Hungarian Standards Board). MSZ: Warsaw, Poland, 2020.
190. PN-B-02867; Ochrona Przeciwpożarowa Budynków—Metoda Badania Stopnia Rozprzestrzeniania Ognia Przez Ściany Zewnętrzne od Strony Zewnętrznej oraz Zasady Klasyfikacji. Polski Komitet Normalizacyjny: Warsaw, Poland, 2013.
191. Franco, A.; Royer-Carfagni, G. Verification formulae for structural glass under combined variable loads. *Eng. Struct.* **2015**, *83*, 233–242. [[CrossRef](#)]
192. Franco, A.; Royer-Carfagni, G. Critical issues in the design-by-testing of annealed glass components. *Eng. Struct.* **2015**, *99*, 108–119. [[CrossRef](#)]

Disclaimer/Publisher’s Note: The statements, opinions and data contained in all publications are solely those of the individual author(s) and contributor(s) and not of MDPI and/or the editor(s). MDPI and/or the editor(s) disclaim responsibility for any injury to people or property resulting from any ideas, methods, instructions or products referred to in the content.